Connectivity in juvenile yellowfin tuna Thunnus albacares between temperate and tropical regions of the western Pacific Ocean

Vol. 713: 151–172, 2023
https://doi.org/10.3354/meps14325

MARINE ECOLOGY PROGRESS SERIES
Mar Ecol Prog Ser

Published June 29

Connectivity in juvenile yellowfin tuna *Thunnus albacares* between temperate and tropical regions of the western Pacific Ocean

Keisuke Satoh[1,*], Satoshi Katayama[2], Toshiyuki Tanabe[3], Kei Okamoto[1]

[1]Fisheries Resources Institute, National Research and Development Agency, Japan Fisheries Research and Education Agency (FRA), 2-12-4 Fukuura, Kanazawa-ku, Yokohama-shi, Kanagawa-ken 236-8648, Japan

[2]Tohoku University Graduate School of Agricultural Science, Aoba-468-1 Aramaki, Aoba Ward, Sendai, Miyagi 980-0845, Japan

[3]Fisheries Resources Institute, National Research and Development Agency, Japan Fisheries Research and Education Agency (FRA), 1551-8, Taira, Nagasaki, Nagasaki 851-2213, Japan

ABSTRACT: Yellowfin tuna *Thunnus albacares* is a commercially important fish species widely distributed between 40° S and 40° N. Mixing rates between tropical and temperate areas of the western Pacific Ocean were investigated using stable carbon ($\delta^{13}C_{otolith}$) and oxygen isotopes ($\delta^{18}O_{otolith}$) in whole otoliths of small juveniles (mean: 5.8 cm standard length, SL) and in otolith cores of large juveniles (32.4 cm SL). The density distribution of $\delta^{18}O_{otolith}$ values for small juveniles showed a significant difference between the areas, whereas patterns for large juveniles were almost identical between areas. In addition, modal values for large juveniles spanned several small juvenile modes. The density distribution of $\delta^{13}C_{otolith}$ values for small juveniles had a single significantly different mode for each area, whereas the distribution of $\delta^{13}C_{otolith}$ values for large juveniles in these areas was bimodal, particularly in the temperate area; these modes corresponded to those for small juveniles in each area. These modal patterns indicate that the majority of large juveniles captured in the temperate area have tropical origins, and mixing from tropical to temperate areas occurs between the areas before recruitment to fisheries in each area. These connectivity patterns during early life history can contribute to refinement of stock assessments of this commercially valuable species.

KEY WORDS: Stable oxygen isotope · Stable carbon isotope · Western Pacific Ocean · Yellowfin tuna

1. INTRODUCTION

In the western and central Pacific Ocean (WCPO), yellowfin tuna *Thunnus albacares* is caught in a broad area from 40° N to 40° S, primarily in tropical areas. Yellowfin tuna is a high-demand species for fisheries and markets. In the last decade (2009–2019), landings of this species have averaged around 0.86 Mt yr^{-1}, making it the second largest tuna fishery in the Pacific Ocean based on FishStatJ (https://www.fao.org/fishery/en/statistics/software/fishstatj). Most of the catch is taken from equatorial areas by large-scale commercial purse seine vessels, longline vessels, pole-and-line vessels, and small-scale vessels with various gear types in Indonesian and Philippine fisheries (Williams & Ruaia 2021). At sizes of approximately 30 cm fork length (FL), yellowfin tuna are captured by purse seine fisheries and small-scale artisanal fisheries. Longline fisheries primarily catch fish larger than 80 cm FL in temperate and tropical areas. The main fishing season for this species is summer in temperate areas in the Northern Hemisphere and year-round in tropical areas. Yellowfin tuna spawn year-round in areas with a sea

*Corresponding author: sato_keisuke31@fra.go.jp

Publisher: Inter-Research · www.int-res.com

surface temperature (SST) of >24°C in the WCPO, with a seasonal pattern for spawning even in tropical regions (e.g. Suzuki 1994).

A stock is a self-contained biological unit in which reproduction, growth, and mortality can be recognized as a single entity, and widely distributed fish populations are known to be composed of several stocks. The stock is a unit for conducting stock assessments and applying management measures, so understanding to which stock the catch belongs is important. A comprehensive review of the stock structure of 4 Pacific tuna species, including yellowfin, indicated that genetic and non-genetic studies supported the presence of discrete stocks in the Eastern Pacific Ocean (EPO) and WCPO, as well as the application potential of fine-scale spatial structuring within each of these regions (Moore et al. 2020).

Numerous tagging experiments on yellowfin tuna in the WCPO (e.g. Hampton & Gunn 1998, Kaltongga 1998, Itano & Holland 2000, Langley et al. 2011, Vincent et al. 2020a,b) have indicated both regional fidelity and long-distance dispersion. Despite some extensive longitudinal and latitudinal dispersion (over 1000 n miles between tagging and recapture location; Langley et al. 2011, Vincent et al. 2020a,b), most recaptures occur closer to the release points, even after a long period of time (Bayliff 1979, 1984, Schaefer & Fuller 2022). Analyses of these spatial patterns have been based on individual fish that are most suitable for physical tagging (larger than 30 cm FL). In particular, the movement traits from hatching to the size at which they are recruited into a fishery have never been studied for this species. In recent years, studies on the nursery origins and movement patterns of tuna species using stable oxygen ($\delta^{18}O_{otolith}$) and carbon isotopes ($\delta^{13}C_{otolith}$) in otoliths have been conducted (Rooker et al. 2008, 2016, Shiao et al. 2009, 2010, Wells et al. 2012). Global records of stable oxygen and carbon isotopes in surface water vary regionally (Chen et al. 2006, LeGrande & Schmidt 2006). Therefore, the chemical composition of otolith isotopes can reflect the area that a fish has occupied (Rooker et al. 2001, 2016, Wells et al. 2012). In previous studies, specimens were collected from commercial fisheries, and the smallest fish in previous studies on tropical tuna in the Pacific Ocean (Wells et al. 2012, Rooker et al. 2016) was approximately 20 cm FL. However, the estimation of mixing rates between tropical and temperate areas for yellowfin tuna at smaller sizes in the WCPO remains unclear. With regard to stock assessment, such information has relevance for how to define fishery regions and stock boundaries. A change in the definition of boundaries could significantly affect the results of tropical tuna stock assessments (Western and Central Pacific Fisheries Commission 2017).

A key question is how a yellowfin population in tropical (hereafter TROP) and temperate areas (hereafter TEM) is connected before recruitment to fisheries (less than approximately 30 cm FL), particularly in the western Pacific Ocean. This study aimed (1) to describe regional changes in stable isotope ratios, (2) to explore relationships between oceanographic conditions and stable isotope ratios, (3) to construct an indicator of nursery grounds of TROP and TEM using stable isotope values of small juveniles collected from both areas, (4) to estimate the mixing rate of large juveniles between areas by applying the indicator, (5) to compare $\delta^{18}O_{otolith}$ and $\delta^{13}C_{otolith}$ for small (ca. 5 cm standard length, SL) and large juveniles (ca. 30 cm SL) between the areas, and (6) to discuss a conceptual model for population connectivity before fishery recruitment in the 2 areas.

2. MATERIALS AND METHODS

2.1. Field sampling and laboratory treatment

In this study, fish samples were divided into 2 categories based on SL: small juveniles (mean: 5.8 cm, range: 2.61–17.8 cm SL), and large juveniles (18.1–49.5 cm SL, Table 1). Samples of small juveniles (n = 175) were collected in both areas (TROP and TEM; Fig. 1) using a mid-water trawl (Tanabe & Niu 1998). The mid-water trawl collection is described briefly here, and in Text S7 in the Supplement (www.int-res.com/articles/suppl/m713p151_supp.pdf). The trawl was towed at 4–5 knots for 30 min at a target depth (TROP: 2 layers at 30–60 and 60–90 m; TEM: 5–35 m; see Table 2). These target depths corresponded with the mixed layer depth and spatial–temporal distribution of small juveniles reported in a previous study (Tanabe 2002). Large juveniles (n = 528) were also collected using commercial purse seine, commercial pole-and-line, and commercial troll fisheries. The sampling area, year, location, number of specimens, length, dates, and gears are shown in Table 1 and Fig. 1. The location for the samples from the purse seine fishery was expressed as the mean longitudinal and latitudinal position of a fishing trip instead of using a set-by-set position in some cases.

Small juveniles caught between 2005 and 2007 were fixed in 99.5% ethanol and those caught in 2011 and 2012 were kept frozen at −30°C. Fish length for both size categories was measured to the nearest 0.1 cm

Table 1. Summary statistics of small and large juvenile of yellowfin tuna *Thunnus albacares* collected in tropical (TROP) and temperate (TEM) areas of the western Pacific Ocean. N: sample size, SL: standard length

	Sampling area	Sampling year	Sampling latitude	Sampling longitude	N	Mean size (cm SL) (SE)	Size range (cm SL) Min	Size range (cm SL) Max	Sampling dates (mo-d) From	Sampling dates (mo-d) To	Sampling gear
Small juveniles	Overall				175	5.8 (0.2)	2.61	17.8			
	TEM	All years	26–30° N	125–130° E	36	9.9 (0.6)	3.18	17.8			
	TEM	2011	28–30° N	128–130° E	18	10.1 (0.8)	4.11	14.1	06-17	07-06	Mid-water trawl
	TEM	2012	26–30° N	125–129° E	18	9.69 (0.2)	3.18	17.8	06-06	06-28	Mid-water trawl
	TROP	All years	6–9° N	138–164° E	139	4.73 (0.12)	2.61	13			
	TROP	2005	4–4° N	145–145° E	14	3.75 (0.14)	2.83	4.8	03-09	03-09	Mid-water trawl
	TROP	2006	6–3° N	162–164° E	7	3.09 (0.17)	2.61	3.66	03-06	03-08	Mid-water trawl
	TROP	2007	4–4° N	138–138° E	4	4.22 (0.24)	3.68	4.77	03-06	03-06	Mid-water trawl
	TROP	2012	2–8° N	146–156° E	36	5.13 (0.37)	3.12	13	12-04	12-12	Mid-water trawl
	TROP	2013	0–9° N	146–156° E	78	4.9 (0.1)	3.09	8.09	11-23	11-30	Mid-water trawl
Large juveniles	Overall				528	32.4 (0.2)	18.1	54.2			
	TEM	All years	24–35° N	122–146° E	251	30.6 (0.4)	18.1	53.6			
	TEM	2011	28–28° N	129–129° E	3	36.5 (0.4)	35.9	37.4	12-05	12-05	Pole and line
	TEM	2013	24–24° N	122–122° E	32	31.1 (0.7)	22.1	37.7	07-27	09-30	Troll
	TEM	2013	35–35° N	146–146° E	13	50.0 (0.5)	46.3	53.6	07-03	07-03	Pole and line
	TEM	2014	24–31° N	122–129° E	117	28.7 (0.5)	18.1	37.2	07-26	09-10	Troll
	TEM	2015	24–24° N	122–122° E	86	29.9 (0.3)	22.7	37.9	06-27	08-21	Troll
	TROP	All years	7–6° N	144–169° E	277	34.0 (0.2)	26	54.2			
	TROP	2011	5–3° N	154–157° E	18	35.1 (1.9)	26.8	54.2	05-06	10-28	Purse seine
	TROP	2013	7–2° N	147–169° E	55	30.5 (0.5)	26	38.6	02-15	12-28	Purse seine
	TROP	2014	6–6° N	144–164° E	117	34.5 (0.2)	26.2	38.5	01-24	12-01	Purse seine
	TROP	2015	6–4° N	148–165° E	87	35.2 (0.3)	28.2	38.1	01-01	12-26	Purse seine

using a caliper. Species identification was performed using a molecular biological technique, namely, multiplex PCR (Higashi et al. 2016), using small portions of each specimen. In previous studies, the length of large juveniles is usually expressed as FL, whereas SL is usually used for small juveniles. In this study, fish length is reported as SL for all specimens. The correction of SL for ethanol fixation of small juveniles and a conversion equation of SL and FL for large juveniles are presented in Text S8. Sagittal otoliths were extracted from specimens, cleaned of biological residue, and then stored in plastic vials with 99.5% ethanol. The left otoliths were used for analysis. The otoliths of large juveniles were embedded in epoxy resin and transversely sectioned, including the primordium, using a diamond-coated blade on a low-speed saw (Isomet1000, Buehler). The sampling path was determined from the core to the ventral and dorsal sides, corresponding to the transverse section of small juvenile otoliths (about 1300 µm width and 300–500 µm depth; Fig. 2). The otolith powder of large juveniles was collected using a micro mill with an antistatic-treated vacuum suction system (Geomil326, Izumo). Approximately half of the otolith powder from otolith sections representing hatch to approximately 9 cm SL was collected from each large juvenile (Fig. 2).

2.2. Oceanographic conditions

To understand the relationships between sea temperature, salinity, and stable isotopes for small juveniles, CTD observations were conducted at each small juvenile sampling station (in 2005 and 2006: SBE19; from 2011 to 2013: SBE911, Sea-Bird Electronics). No data for sea temperature and salinity were collected in 2007. The actual sampling layer of the mid-water trawl in TROP from 2005 to 2007 was 0–200 m; however, juvenile *Thunnus* spp. (mostly

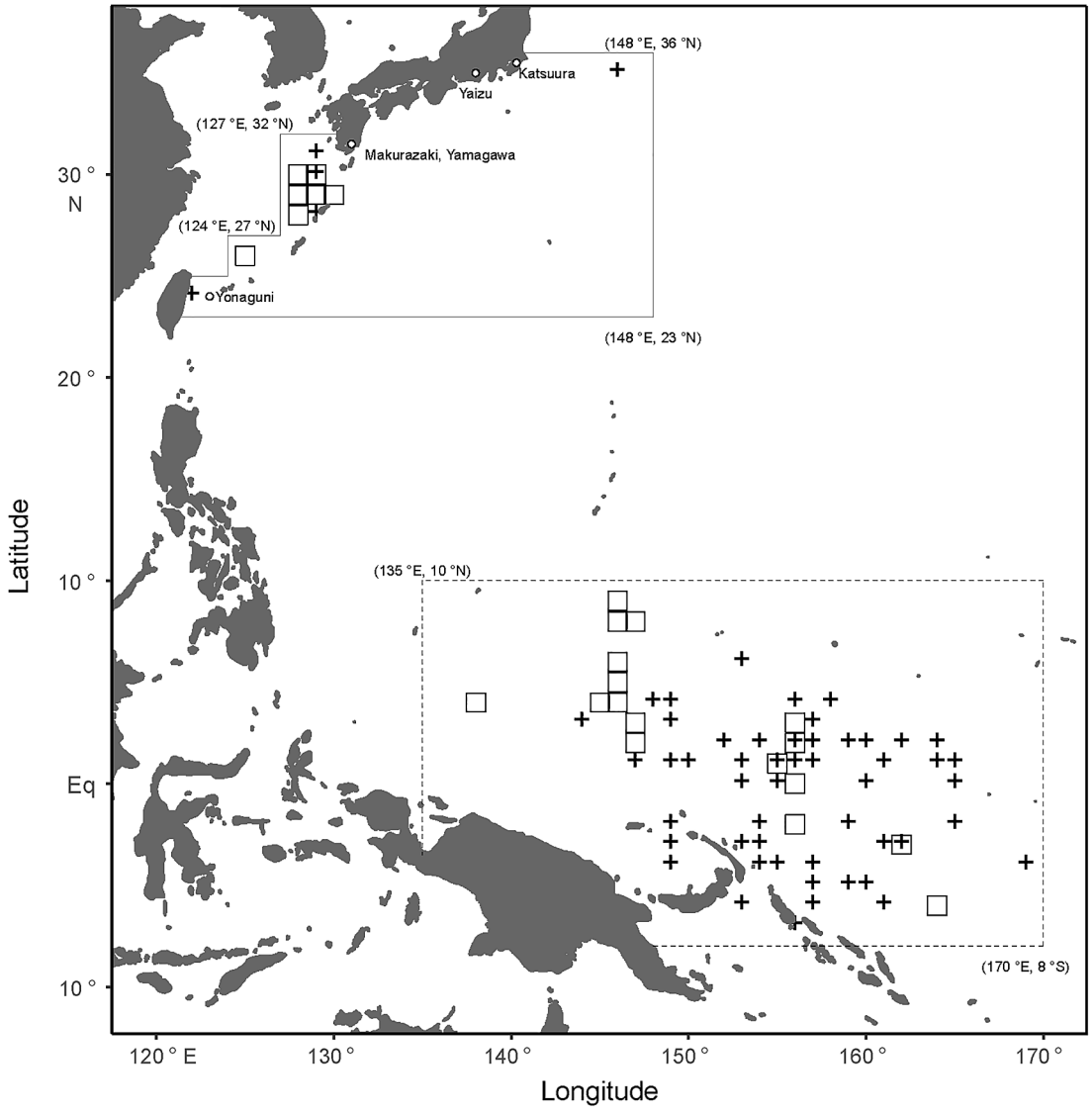

Fig. 1. Sampling sites for yellowfin tuna *Thunnus albacares*. Fish were collected by size. Crosses: large juveniles; open squares: small juveniles; open circles: sampling ports. The areas surrounded by a solid line and dashed line define the temperate (TEM) and tropical (TROP) areas, respectively, for the average sea temperature and salinity shown in Fig. 3

yellowfin tuna) were primarily distributed at depths shallower than 100 m, as observed by mid-water trawls in the tropical areas of the western Pacific Ocean (Tanabe 2002). Thus, oceanographic conditions at a depth of 30–90 m are presented, and compared among the years sampled.

The sea temperature and salinity for large juveniles were not available for each collection date and place. In addition, sea temperature and salinity over a broad spatial range were investigated using the monthly mean potential temperature and salinity at a resolution of 20 min (1/3rd degree) latitude and 60 min (1 degree) longitude obtained from the NOAA NCEP Global Ocean Data Assimilation System (www.esrl.noaa.gov/psd/data/gridded/data.godas.html). The oceanographic conditions for large juveniles in each area were compiled to mimic the sampling layers of small juveniles, and the Southern Oscillation Index was obtained from the website of the Japan Metrological Agency (https://ds.data.jma.go.jp/tcc/tcc/products/elnino/index/soi). The methodology is described in detail in Text S10.

2.3. Stable isotope measurement

The carbon and oxygen isotope compositions of the powdered otolith materials were analyzed using a

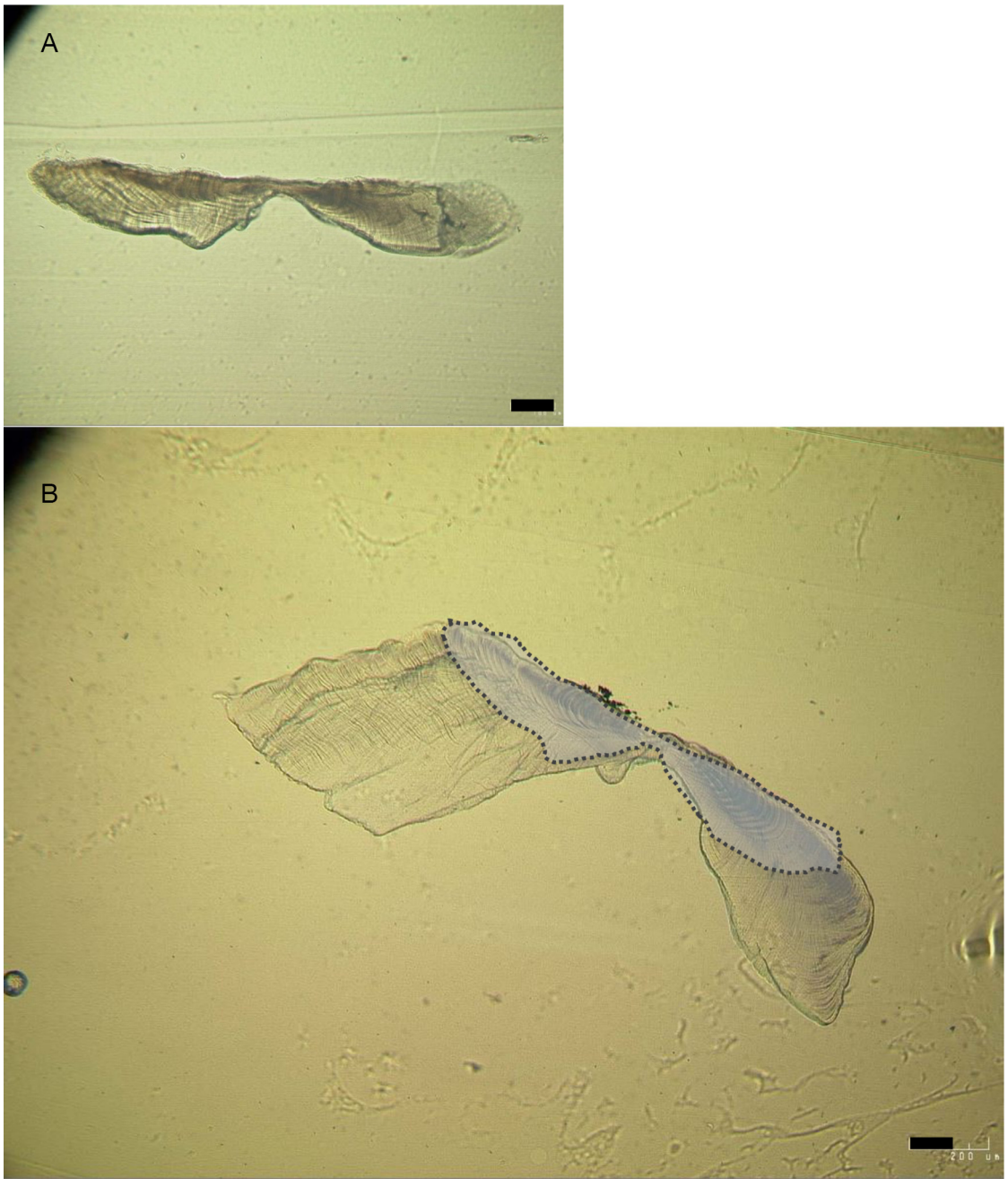

Fig. 2. Transverse cross-sections of sagittal otoliths for (A) small juvenile (8.9 cm standard length, SL) and (B) large juvenile (36.4 cm SL) yellowfin tuna *Thunnus albacares*. Otolith-milled samples for large juveniles were obtained from the shaded area in (b), which is the shape of small juvenile otoliths (A). Scale bars in both panels = 100 µm

DELTA Plus Advantage mass spectrometer (Thermo Finnigan Electron). CO_2 for isotope measurements was produced in a reaction with pure orthophosphoric acid at 28°C, which was added to the samples in individual reaction vials. The long-term reproducibility of the DELTA Plus Advantage mass spectrometer for $\delta^{18}O$ and $\delta^{13}C$ (1 SD) was more than ±0.1‰ for this experiment. All isotope values are reported in accordance with the standards of the International Atomic Energy Agency, Vienna. The otolith $\delta^{18}O$ and $\delta^{13}C$ values are reported in standard δ notation relative to Pee Dee belemnite through calibration against an NBS19 standard:

$$\delta = (R\_sample - R\_standard)/R\_standard \times 1000\ (‰) \quad (1)$$

where R is the ratio ^{18}O:^{16}O or ^{13}C:^{12}C in the sample or standard.

2.4. Statistical analysis

Relationships between the stable isotopes and salinity, sea temperature, year sampled, SL, latitude, and longitude in each area were first explored using box plots and regression analysis. The results are described in Text S1–S5 and Figs. S1–S7. Multivariate analysis of variance (MANOVA) was then used to test the differences in $\delta^{13}C_{otolith}$ and $\delta^{18}O_{otolith}$ of small juveniles and large juveniles among the areas (TEM and TROP) and sampling years. Pillai's trace statistic was used to determine significance. A post hoc multiple comparison was conducted using the Tukey–Kramer test. Univariate tests for $\delta^{13}C_{otolith}$ and $\delta^{18}O_{otolith}$ were also performed using a generalized linear model (GLM). In forming an indicator (classification model) for the nursery grounds (TEM or TROP), a general additive model (GAM) from the 'mgcv' library (R Core Team 2021) was applied to $\delta^{13}C_{otolith}$ and $\delta^{18}O_{otolith}$ of small juveniles. The classification success rate (%) for small juveniles was simply calculated as 100 minus the classification error rate. In preliminary analysis, other discriminant analyses, including support vector machine with 3 other kernel types (linear, quadratic, and radial basis), linear discriminant function analysis, quadratic discriminant function analysis, and logistic discriminant analysis were also conducted. After comparing the classification rate among these models, GAM was selected because of its better performance with regard to the overall classification success rate and for each area's classification rate in TEM and TROP. Details about the model selection process are provided in Text S6. The developed discriminant GAM using small juvenile data was applied to the stable isotopes of large juveniles to investigate the mixing rate between TEM and TROP. The mixing rate of large juveniles is presented as a percentage of fish originating from TROP (e.g. fish estimated to hatch in TROP). The homogeneity of covariance and normality of $\delta^{18}O_{otolith}$ and $\delta^{13}C_{otolith}$ among the groups tested was examined using the *F*-test and Shapiro–Wilk test, respectively. The homogeneity of covariance was satisfied for both stable radio isotopes. The normality assumption was violated only for $\delta^{18}O_{otolith}$; thus, a Yeo–Johnson power transformation (Yeo & Johnson 2000) was used to improve normality, which can be applied to a negative value. However, the transformed values still violated the normality assumption. $\delta^{18}O_{otolith}$ was not transformed for further analysis. Pillai's trace statistic was considered the most robust among the MANOVA tests, with adequate power to detect true differences in a variety of situations (Olson 1974). These statistical analyses were performed using SAS (v9.4, SAS Institute) and R (R Core Team 2021).

A larval database was used to understand the spatial coverage of the small juveniles sampled in this study relative to the whole distribution of small juveniles. The database was constructed by the Fisheries Resources Institute, National Research and Development Agency, Japan Fisheries Research and Education Agency (FRA); this database contained the sampling date, location, and number of tuna larvae of each plankton net tow. These samplings were conducted by fishery training vessels as well as local and national governmental fishery research vessels in Japan from 1956 to 1998, which recorded 51 121 plankton net tows in the Pacific Ocean. Some of these results were summarized as atlases for the geographical distribution of tuna species larvae and published previously (Nishikawa et al. 1985). In addition, yellowfin tuna larvae grow to nearly 13 mm SL in 20 d, when they are termed juveniles (Okiyama 1988, Wexler et al. 2007), as their number of dorsal fin rays and anal fin rays reaches the same number found in adult fish. A bias in the geographical distribution of this historical sampling effort was noted by the authors (Nishikawa et al. 1985). A relatively large number of plankton net samples were from areas where a relatively large number of larvae were collected, such as the southern part of the TEM and fishing training grounds in subtropical areas of the central Pacific Ocean. Moreover, high larval catch occasionally occurred in areas with low sampling effort, reflecting the patchy distribution of tuna larvae (Satoh 2010). Therefore, larval density, excluding an area where few plankton net tows were conducted, serves as a basis of the larval distribution of this species instead of using the catch number itself. Bootstrap analysis was conducted to assess the robustness of the estimated larval density patterns. A stratum was defined as a latitude and longitude of 5° × 5° per month, compiling the number of plankton net tows in a stratum; the stratum was then deleted from this analysis if the number of tows was <10 mo^{-1}. In making a bootstrap sample, 50 random samplings with replacement were conducted in each stratum. Bootstrap samplings were repeated 1000 times, and the mean number of larvae per plankton net tow in each stratum was calculated on the basis of the 1000 bootstrap samples. In this analysis, TEM and

TROP were defined from 120–150° E, 20–40° N, and 135–170° E, 10° S to 10° N, respectively; the defined area shown in Fig. 1 was not used because of differences in the spatial resolution of the data. The areas outside of TEM and TROP and east of 180°E were defined as 'others'. The monthly larval density by area (TEM, TROP, and others) was defined as the area-weighted larval density, which is a product of the monthly average number of larvae per plankton net tow and monthly number of cells (5° × 5°).

2.5. Sensitivity analysis

A series of sensitivity analyses was conducted to understand the length effect on the classification success rate of small juveniles and the mixing rate (percentage of individuals originating in TROP) of large juveniles in discriminant analyses using GAM. Three scenarios were proposed. (1) A significant correlation was observed between the SL of small juveniles and $\delta^{18}O_{otolith}$, and the mean fish length in TEM was significantly larger than that in TROP in exploratory analysis. This raised the concern that the differences in $\delta^{18}O_{otolith}$ between areas might be due to the differences in fish length. Scenario (2), the length of the smallest large juvenile (18.1 cm SL) was close to that of the largest small juvenile (17.8 cm SL). This raised a concern because of the possible breach of the assumption for discriminant analysis, that is, small specimens were collected from their nursery grounds. Scenario (3) was to try to detect when the small juveniles moved from their hatching area to another area. These 3 scenarios were investigated by controlling the size range of the specimens used in analysis: (1) from 5 to 40 cm SL, (2) under 12 cm SL and above 25 cm SL, and (3) in 1 cm intervals from 2 to 18 cm SL.

3. RESULTS

3.1. Field sampling, sea temperature, and salinity

The number of small juvenile specimens in TEM and TROP used for stable isotope analysis was 36 and 139, respectively. Sampling in TEM was conducted in June or July, whereas that in TROP was conducted in March from 2005 to 2007, October in 2012, and December in 2013 (Table 1, Fig. 1). The mean SL of small juveniles in TEM (mean ± SE: 9.9 ± 0.6 cm, range: 3.18–17.8 cm) was significantly larger than that in TROP (4.73 ± 0.12 cm, range: 2.61–13 cm SL; $F_{1,173} = 184$, $p < 0.001$; Table 1). The sea temperature was higher in TROP (28.8 ± 0.03°C) than in TEM (27.0°C ± 0.03°C; Table 2). Salinity was higher in TROP (34.5 ± 0.01 psu) than in TEM (34.1 ± 0.01 psu). The ranges of sea temperature and salinity were similar among the years sampled in each area; however, in 2006, a relatively low sea temperature (27.9°C) was observed in TROP.

Sampling of large juveniles was carried out year-round in TROP, whereas large juveniles were collected from July to September in TEM, except for 3 specimens in December 2011 (Table 1). The number of large juvenile specimens in TEM and TROP was 251 and 277, respectively. The mean SL of large juveniles collected in TEM (30.6 ± 0.4 cm) was significantly smaller than that in TROP (34.0 ± 0.2 cm; $F_{1,526} = 57.89$, $p < 0.001$; Table 1). In TROP, the mean sea temperature and salinity during the study period were 28.7°C and 34.7 psu (Fig. 3). The sea temperature in TROP substantially decreased after August 2014, reaching 27.5°C in 2015. In contrast, salinity increased to more than 35.0 psu in 2015. These drastic changes in oceanographic conditions corresponded to El Niño after June 2014 (Table S1). In TEM, mean sea temperature and salinity during the study period were 23.7°C and 34.7 psu. No clear relationship was observed between time series changes and El Niño in TEM.

The number of small juvenile sampling stations for this analysis in TEM and TROP was 22 and 25, respectively. Across all sampling stations, the relationship between oceanographic conditions and $\delta^{13}C_{otolith}$ was significantly positive (salinity: 0.467‰ increase per 1 psu increase, $p = 0.001$; sea temperature: 0.244‰ increase per 1°C increase, $p < 0.001$), although their R-squared values were low (salinity: 0.0569; sea temperature: 0.208; Fig. 4). Significantly negative relationships between the oceanographic conditions and $\delta^{18}O_{otolith}$ were found (salinity: 0.534‰ decrease per 1 psu increase, $p < 0.001$; sea temperature: 0.189‰ decrease per 1°C increase, $p < 0.001$).

3.2. Stable isotopes of small and large juveniles

The $\delta^{13}C_{otolith}$ and $\delta^{18}O_{otolith}$ values of small juveniles were significantly different between the 2 areas (TEM and TROP; MANOVA, $F_{2,166} = 45.15$, $p < 0.001$; Table 2, Fig. 5). The mean ± SE $\delta^{13}C_{otolith}$ of small juveniles from TEM (–10.6 ± 0.1) was significantly lower than that from TROP (–9.86 ± 0.04; $p < 0.001$). In addition, the $\delta^{18}O_{otolith}$ of small juveniles in TEM (–2.26 ± 0.06) was significantly higher than that in

Table 2. Mean and range of otolith carbon ($\delta^{13}C$) and oxygen ($\delta^{18}O$) stable isotope values of small juvenile of yellowfin tuna *Thunnus albacares* by area and sampling year collected from the western central Pacific Ocean. The classification success rate (%) by area and year was estimated using a general additive model. Mean and range of sea temperature (°C) and salinity observed by a CTD probe for each mid-water trawl survey. NA: not available; N: sample size. The sampling layer for temperate (TEM) and tropical (TROP) areas was 5–35 m and 30–90 m depth, respectively

Sampling area	Sampling year	$\delta^{13}C_{otolith}$			$\delta^{18}O_{otolith}$			N	Classification success rate (%)	Sea temperature			Salinity		
		Mean (SE)	Min	Max	Mean (SE)	Min	Max			Mean (SE)	Min	Max	Mean (SE)	Min	Max
	Overall							175	90.7						
TEM	All years	–10.6 (0.1)	–11.6	–9.42	–2.26 (0.06)	–3.46	–1.64	36	72.2	27.0 (0.03)	24.3	28.2	34.1 (0.02)	22.4	34.7
TEM	2011	–10.5 (0.1)	–11.4	–9.42	–2.28 (0.09)	–3.46	–1.96	18	66.7	26.9 (0.1)	24.6	28.2	34.2 (0.02)	33.4	34.7
TEM	2012	–10.7 (0.1)	–11.6	–9.88	–2.24 (0.09)	–3.19	–1.64	18	77.8	27.1 (0.03)	24.3	28.1	34.0 (0.03)	22.4	34.7
TROP	All years	–9.86 (0.04)	–10.9	–9.04	–2.68 (0.03)	–3.74	–1.96	139	96.5	28.8 (0.03)	24.9	30.8	34.5 (0.01)	33.9	35.5
TROP	2005	–9.62 (0.06)	–9.92	–9.31	–2.78 (0.04)	–3.02	–2.48	14	NA	29.8 (0.04)	28.8	30.0	34.6 (0.04)	34.3	35.1
TROP	2006	–9.99 (0.10)	–10.3	–9.67	–2.71 (0.10)	–3.08	–2.29	7	NA	27.9 (0.1)	24.9	30.4	34.6 (0.02)	34.1	35.2
TROP	2007	–9.31 (0.15)	–9.69	–9.04	–2.82 (0.29)	–3.67	–2.42	4	NA	NA	NA	NA	NA	NA	NA
TROP	2012	–9.77 (0.07)	–10.6	–9.07	–2.68 (0.04)	–3.09	–2.24	36	100.0	29.0 (0.03)	26.6	30.3	34.5 (0.02)	33.9	35.5
TROP	2013	–9.96 (0.05)	–10.9	–9.07	–2.66 (0.04)	–3.74	–1.96	78	94.9	29.2 (0.04)	26.9	30.8	34.5 (0.02)	33.9	35.4

TROP (–2.68 ± 0.03; $p < 0.001$). The $\delta^{13}C_{otolith}$ and $\delta^{18}O_{otolith}$ of small juveniles collected from TEM did not show significant annual differences ($F_{2,30} = 1.21$, $p = 0.313$; Table 2, Fig. 6). No significant annual differences in $\delta^{18}O_{otolith}$ of small juveniles collected from TROP were observed, with low variability among the years. The $\delta^{13}C_{otolith}$ of small juveniles collected from TROP did not show significant annual differences among 2006, 2012, and 2013 (Table 2, Fig. 6). To match the sampling years for large juveniles, a subset of small juvenile specimens (2011 and 2012 from TEM; 2012 and 2013 from TROP) were used to develop a GAM for classification and to avoid the potential to confound temporal differences with spatial differences in the classification model (Fig. 7). The classification success rate between the 2 areas (TEM and TROP) was 90.7%, and the classification success rates in TEM and TROP were 72.2 and 96.5%, respectively (Table 2).

The relationships between stable isotopes and 4 other factors, i.e. SL, sampling year, latitude, and longitude, were explored to investigate the possibility that the differences in these isotopes were derived from the effects of these factors instead of the effect of differences in area. This exploratory analysis and further GLM results are shown in detail in Texts S1–S5 and Figs. S1–S7. Factors, including all 4 abovementioned factors, should be considered as covariates for further analysis unless specifically mentioned. SL was treated as a categorical variable, such as the smallest (<5 cm SL) or the largest length group (>40 cm SL). For large juveniles, the least square means of $\delta^{13}C_{otolith}$ and $\delta^{18}O_{otolith}$ by longitude in this analysis showed 0.0241‰ and 0.0201‰ increase per 1° longitudinal change, respectively, from 147.5 to 167.5° E.

Mean fish length in the matched (i.e. sampled area and discriminated area are the same) and mismatched groups was investigated to examine the appropriateness of the assumption that small juvenile specimens were collected from their hatch areas. In TEM, 26 of 36 individuals were discriminated as the matched group. The average SL of the matched group was 10.9 cm SL, which was significantly larger than that of the mis-matched group (7.08 cm SL, n = 10; $F_{1,34} = 11.38$, $p = 0.001$). The specimens in the mismatched group were collected in multiple years, and their mean length was not different (2011: 7.52 cm SL, n = 6; 2012: 6.43 cm SL, n = 4). In TROP, 114 specimens were discriminated as the matched group. The average SL of the matched group was 5.44 cm SL (n = 110), which was not significantly different from that of the mis-matched group (4.96 cm SL, n = 4; $F_{1,112}$ =

0.442, p = 0.507). Despite a significant difference between the mean lengths of the 2 groups in TEM, the mean SL in the 2 groups was similar every 2 years (not shown). A larger small juvenile in TEM is not necessarily a fish determined from TROP, and a similarity in length range was observed between the matched and mis-matched groups.

The $\delta^{13}C_{otolith}$ and $\delta^{18}O_{otolith}$ values of large juveniles were significantly different between the 2 areas (TROP and TEM; MANOVA, $F_{2,521} = 49.76$, $p < 0.001$), although both isotopes showed very similar distributions except for $\delta^{13}C_{otolith}$ in 2013 (Table 3, Fig. 6). The $\delta^{13}C_{otolith}$ of large juveniles from TEM (–10.2 ± 0.03) was significantly lower than that from TROP (–9.78 ± 0.04; $p < 0.001$), while the $\delta^{18}O_{otolith}$ of large juveniles from TEM (–2.55 ± 0.03) was not significantly different from TROP (–2.6 ± 0.03; p = 0.177).

The classification model was applied to the large juveniles only from 2013 and 2014. These large juveniles are part of the same cohort as the small juveniles from 2011 to 2013 that form the baseline for our classification model (Fig. 8). The percentage of large

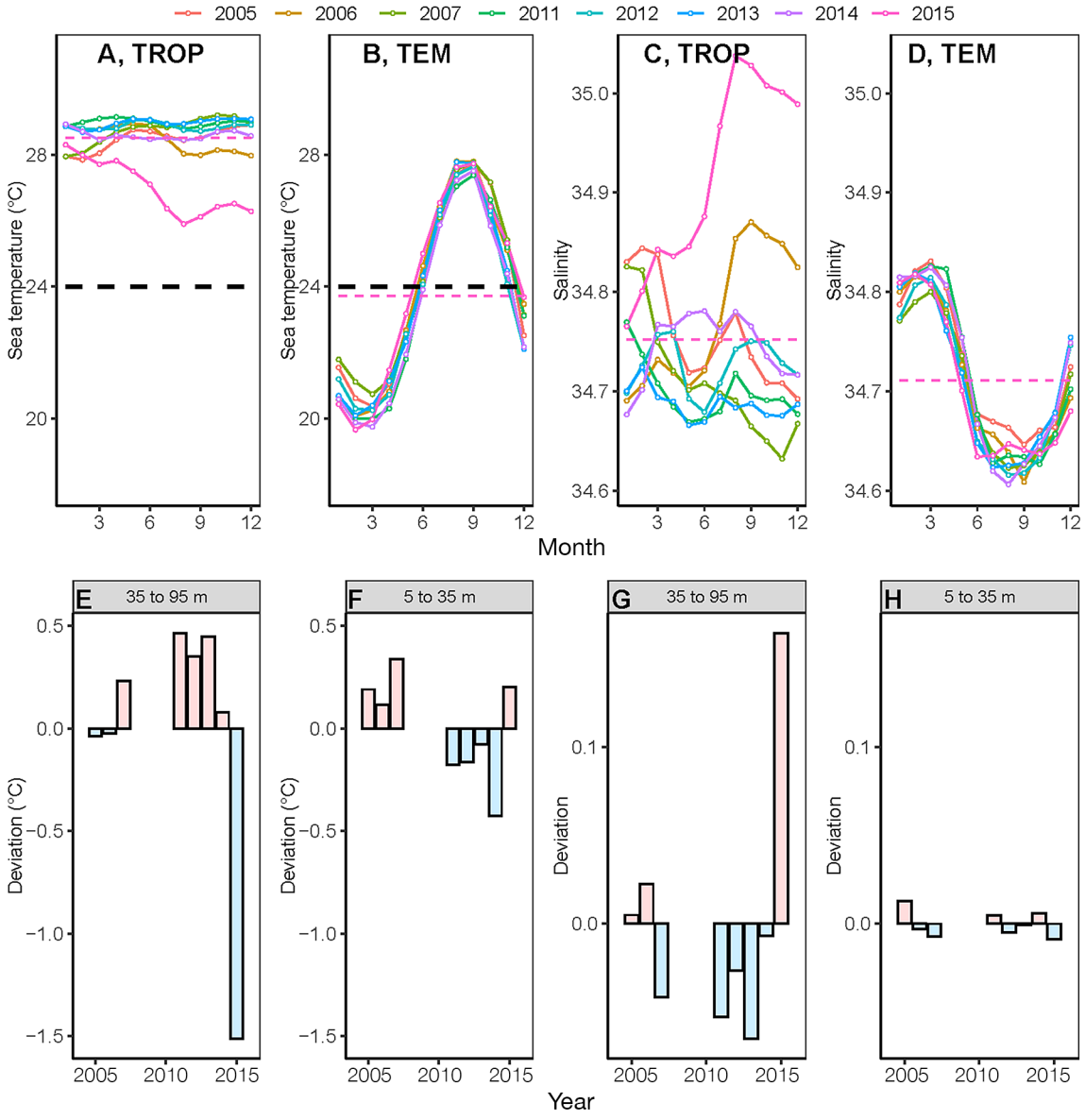

Fig. 3. (A,B) Sea temperature and (C,D) salinity in tropical (TROP: 35–95 m depth) and temperate (TEM: 5–35 m depth) areas from 2005 to 2015 by month for each year. The red dashed lines indicate the average values from 2005 to 2015 in each area; the black dashed lines indicate the approximate low temperature limit of the larval occurrence of yellowfin tuna (24°C). (E–H) Annual temperature deviations (°C) from average values for 2005 to 2015. The area delineations of TEM and TROP are shown in Fig. 1

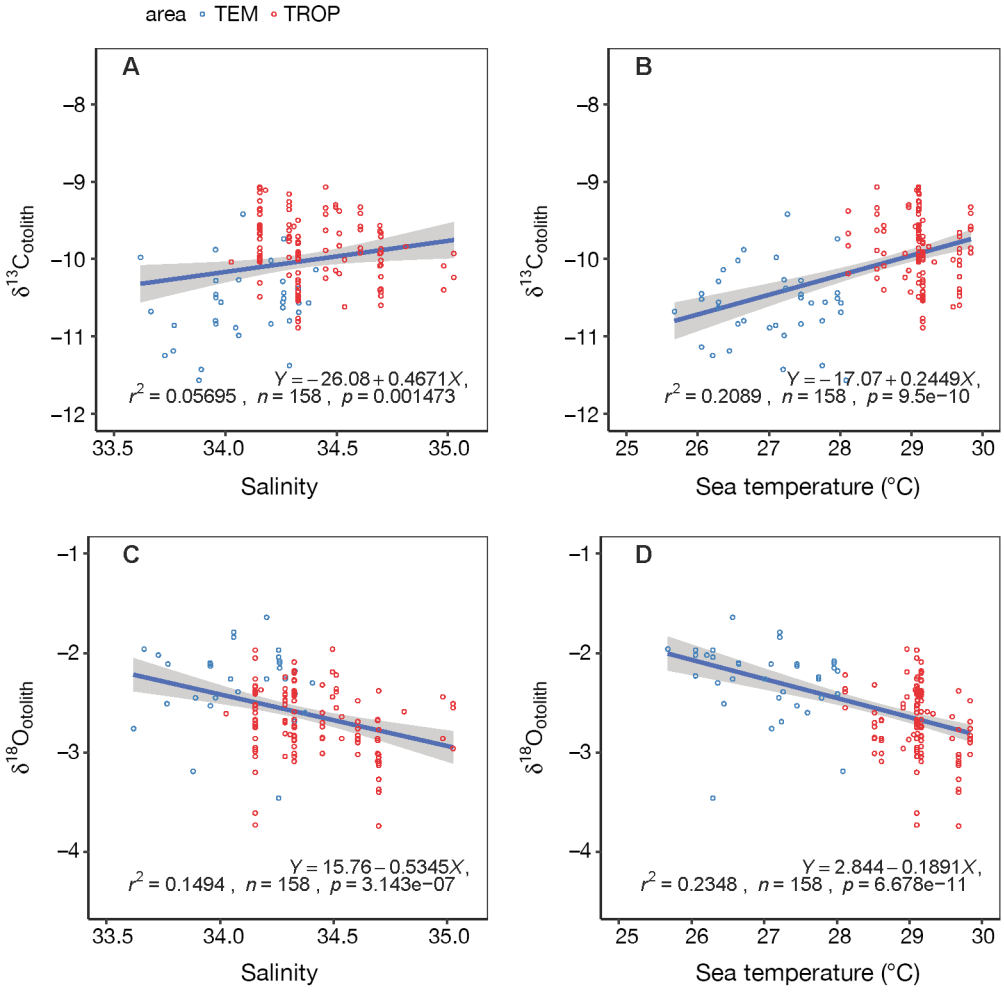

Fig. 4. Relationship between oceanographic conditions (sea temperature and salinity) and otolith (A,B) carbon ($\delta^{13}C_{otolith}$) and (C,D) oxygen ($\delta^{18}O_{otolith}$) stable isotope values of yellowfin tuna *Thunnus albacares* by area (TEM: temperate, TROP: tropical) in the western and central Pacific Ocean. Blue lines indicate regression line, and shaded areas indicated 95% CI of the regression line

juveniles originating from tropical areas (i.e. a fish estimated to hatch in TROP) was 95.9% for those collected in TROP and 78.4% for those collected in TEM (Table 3). The point estimates of the percentage in TROP were always higher than those in TEM in the 2 years (Table 3, Fig. 9). The percentage in TROP from June to August was slightly lower than that in other months.

The density distribution of $\delta^{13}C_{otolith}$ values for small juveniles showed a significant difference between the areas, whereas the distribution of $\delta^{13}C_{otolith}$ for large juveniles in the areas was bimodal, particularly in TEM. Notably, each mode in the bimodal pattern for large juveniles in TEM corresponded to the modes of small juveniles in each area. The bimodal pattern of large juveniles in TROP was detectable but weak. This bimodal pattern of large juveniles for $\delta^{13}C_{otolith}$ values was still detected in TEM by sampling year (blue arrows in Fig. 6F,P,T). Although no bimodal pattern was observed in 2013, the distribution of $\delta^{13}C_{otolith}$ showed a wide peak similar to the integrated 2 modes (Fig. 6N).

The density distribution of $\delta^{18}O_{otolith}$ for small juveniles showed a significant difference between TROP and TEM, whereas that of $\delta^{18}O_{otolith}$ for large juveniles in the 2 areas was almost identical; their modes of large juveniles were distributed around the midpoint of small juvenile modes (Fig. 5). The similarity of $\delta^{18}O_{otolith}$ in both areas for large juveniles was also detected when broken down per sampling year (Fig. 6). $\delta^{18}O_{otolith}$ for large juveniles per year resembled that between the 2 areas for all sampled years; a sharp spike in 2011 (Fig. 6E), a broad distribution in 2013 (Fig. 6M), and a single mode in 2014 (Fig. 6O) and 2015 (Fig. 6S) were found. In contrast, for small juveniles, no such similarity in $\delta^{18}O_{otolith}$ density distribution was observed between the 2 areas.

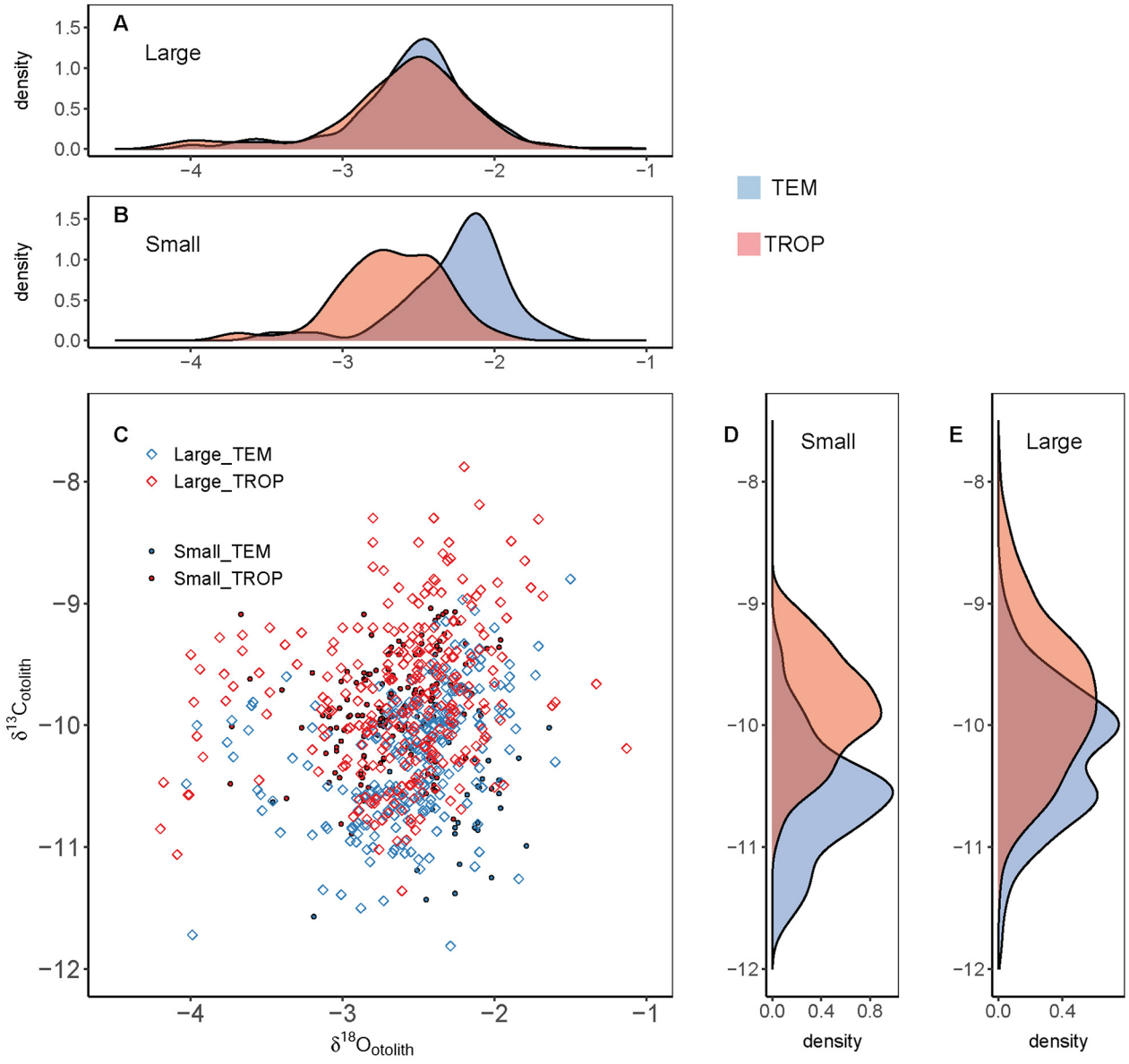

Fig. 5. Density plots of otolith carbon ($\delta^{13}C_{otolith}$) and oxygen ($\delta^{18}O_{otolith}$) stable isotopes of yellowfin tuna *Thunnus albacares* by fish size (small and large juveniles) and area (TEM: temperate, TROP: tropical) in the western central Pacific Ocean. Oxygen ($\delta^{18}O_{otolith}$) stable isotope for (A) large juveniles and (B) small juveniles and carbon ($\delta^{13}C_{otolith}$) stable isotope for (D) small juveniles and (E) large juveniles. (C) Scatter plot for all sizes and areas combined

3.3. Using spawning ground and season to understand the coverage of juvenile sampling

The number of strata defined by unique 5° × 5° cells and months sampled in the original larval database was 1189. It decreased to 591 when a stratum was omitted because of low effort (<10 samples) (Fig. 10), and the number of samples decreased from 27 525 to 24 925. Based on bootstrap analysis using the FRA larval database (Nishikawa et al. 1985), the average area-weighted larval density in TEM was 8.341 larvae per tow. The monthly values ranged from 0.0376 to 23.7, with a peak from May to July (12.2, 23.7, and 5.55; Fig. 10). In TROP, the average density was 4.34; larvae occurred year-round, except for March, with seasonal peaks from April to May (0.243 and 5.83) and from October to December (10.4, 19.1, and 5.80; Fig. 10). For others outside of TEM and TROP, the average density was 4.12. The month sampled for small juveniles in this study had the highest larval density (Table 1). The total density (summing up the area-weighted larval density) for TEM, TROP, and 'others'

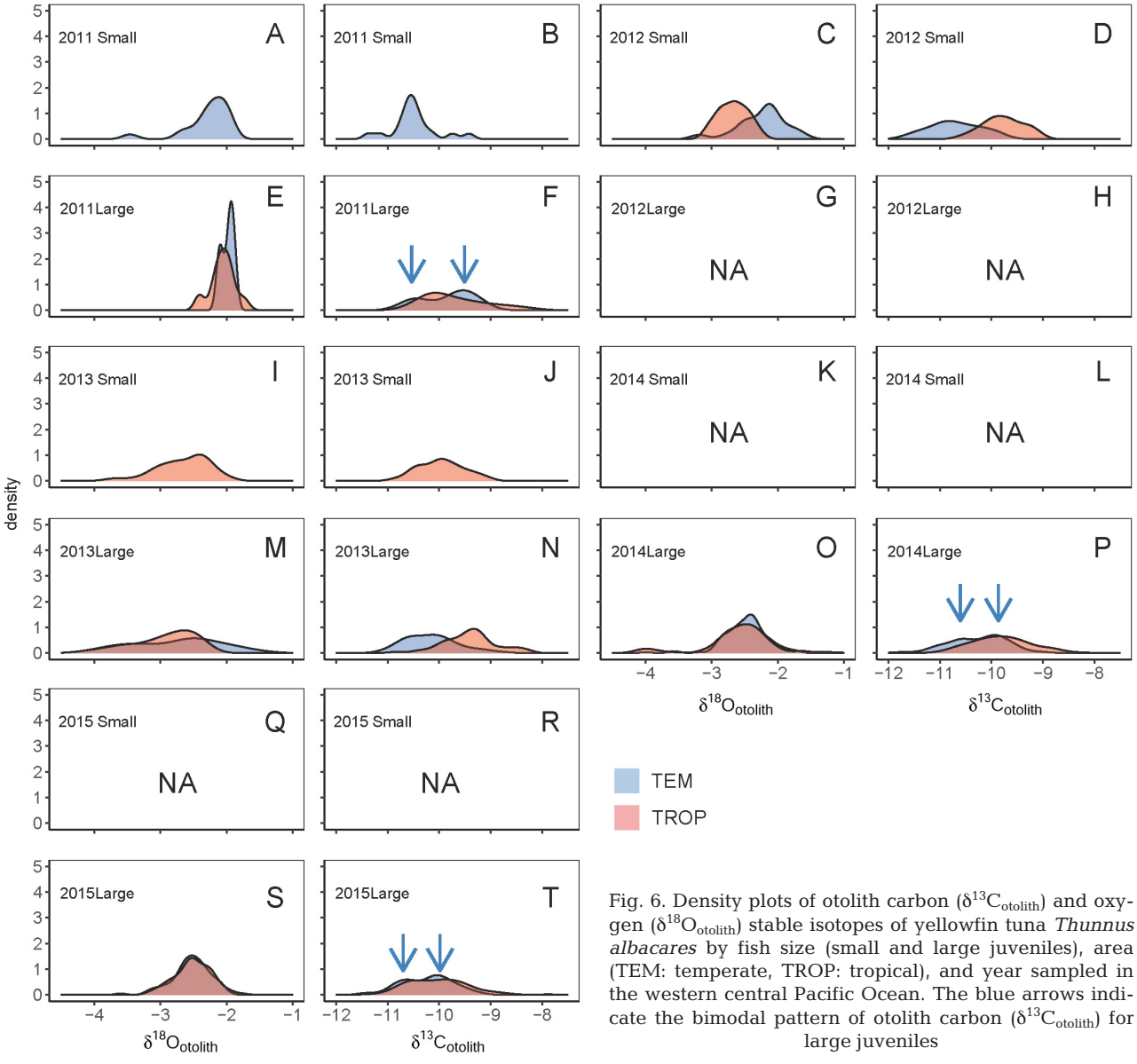

Fig. 6. Density plots of otolith carbon ($\delta^{13}C_{otolith}$) and oxygen ($\delta^{18}O_{otolith}$) stable isotopes of yellowfin tuna *Thunnus albacares* by fish size (small and large juveniles), area (TEM: temperate, TROP: tropical), and year sampled in the western central Pacific Ocean. The blue arrows indicate the bimodal pattern of otolith carbon ($\delta^{13}C_{otolith}$) for large juveniles

was 41.7, 47.8, and 49.4, respectively. The coverage of the months sampled for TEM and TROP (TEM: June and July; TROP: November and December) was estimated to be 70.3% and 52.1% within each area, respectively. Considering the occurrence of larvae outside of TROP and TEM, 39.0% of larvae from the whole WCPO (east of 180° E) were targeted in the area and month sampled in this study.

3.4. Sensitivity analysis

In Scenario (1) (see Section 2.5), the number of small juveniles was reduced from the original dataset (from 150 to 82; Tables 2 & 4). In addition, the classification success rate for TEM was improved (from 72.2 to 83.3%), and the change in the classification success rate for TROP was not large (from 96.5 to 96.2%). In the second scenario, the reduction in small juvenile specimens in TEM was large (from 36 to 24), and the classification success rate decreased (from 72.2 to 66.7%). The mixing rate of large juveniles for scenarios 1 (91.5%) and 2 (92.0%) was close to the original value (90.7%). The third sensitivity analysis tested the assumption of discriminant analysis in this study, which assumed that the small juveniles were collected from their hatch area. If this assumption is true, then the classification success rate of small juveniles has a high value when fish are small (clearly divided between areas), and it

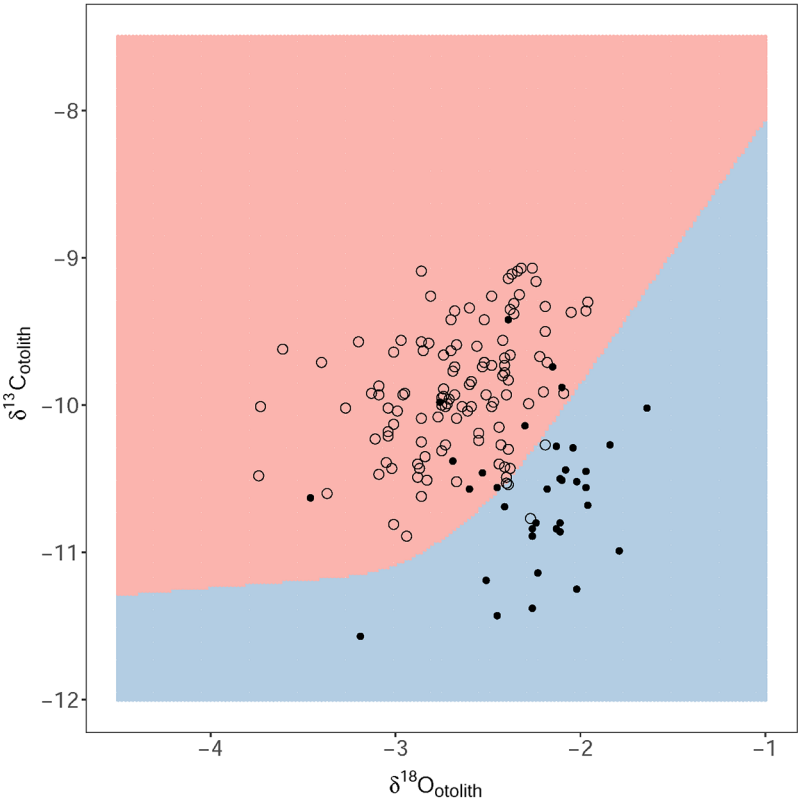

Fig. 7. Otolith carbon ($\delta^{13}C_{otolith}$) and oxygen ($\delta^{18}O_{otolith}$) of small juvenile yellowfin tuna *Thunnus albacares* by area in the western and central Pacific Ocean. Solid and open circles indicate the specimens caught in temperate and tropical areas, respectively. Blue and red shaded areas represent the classified areas (estimated nursery ground) of temperate and tropical areas, respectively, based on the generalized additive model

decreases (less divided) in accordance with their growth, particularly when the upper limit of the SL range increases. The classification success rate from 2 to 6 cm SL in TROP decreased, but in TEM success first decreased to 6 cm and then increased again (Fig. 11). These results suggest that the limited size range may emphasize the effect of differences between the 2 areas; thus, the results are not conclusive.

4. DISCUSSION

4.1. Regional changes in stable isotopes

Whether the regional patterns of $\delta^{13}C_{otolith}$ and $\delta^{18}O_{otolith}$ in this study matched the spatial distribution of $\delta^{13}C_{seawater}$ and $\delta^{18}O_{seawater}$ and $\delta^{13}C_{otolith}$ and $\delta^{18}O_{otolith}$ in previous studies remains a question. The magnitude of stable isotope values of small and large juveniles was in the range of the reported mean values for young-of-the-year yellowfin tuna in tropical and sub-tropical areas of the Pacific Ocean ($\delta^{13}C_{otolith}$: −10.56 to −9.32; $\delta^{18}O_{otolith}$: −2.87 to −1.69) (Rooker et al. 2016). Chen et al. (2006) reported an increasing longitudinal variation in $\delta^{13}C_{seawater}$ from the west to the east Pacific Ocean. The zonal pattern matches the results of the present study, from 145 to 170° E for large juveniles in the TROP. The difference in $\delta^{13}C_{otolith}$ between the Philippines and Solomon Islands was 0.90‰ in

Table 3. Mean and range for otolith carbon ($\delta^{13}C$) and oxygen ($\delta^{18}O$) stable isotope values of large juvenile of yellowfin tuna *Thunnus albacares* by area (TEM: temperate; TROP: tropical) and year sampled; these were collected from the western central Pacific Ocean. The percentage of large juveniles originating from the tropical areas (%) by area and year was estimated using a general additive model. N: sample size. NA: not available

Sampling area	Sampling year	$\delta^{13}C_{otolith}$			$\delta^{18}O_{otolith}$			N	% originating in TROP
		Mean (SE)	Min	Max	Mean (SE)	Min	Max		
	Overall							528	87.4
TEM	All years	−10.2 (0.03)	−11.8	−8.8	−2.55 (0.03)	−4.03	−1.5	251	78.4
TEM	2011	−9.84 (0.33)	−10.5	−9.37	−1.99 (0.06)	−2.1	−1.9	3	NA
TEM	2013	−10.2 (0.1)	−11.1	−8.8	−2.75 (0.10)	−4.03	−1.5	45	91.1
TEM	2014	−10.3 (0.1)	−11.8	−8.97	−2.49 (0.03)	−3.99	−1.71	117	73.5
TEM	2015	−10.2 (0.1)	−11.4	−9.18	−2.54 (0.03)	−3.6	−2	86	NA
TROP	All years	−9.78 (0.04)	−11.4	−7.88	−2.6 (0.03)	−4.2	−1.13	277	95.9
TROP	2011	−9.69 (0.15)	−10.5	−8.31	−2.06 (0.04)	−2.41	−1.71	18	NA
TROP	2013	−9.41 (0.07)	−10.8	−8.3	−2.95 (0.06)	−4.2	−2.3	55	100
TROP	2014	−9.8 (0.1)	−11.1	−8.19	−2.59 (0.05)	−4.18	−1.13	117	94
TROP	2015	−10.0 (0.1)	−11.4	−7.88	−2.5 (0.03)	−3.16	−1.76	87	NA

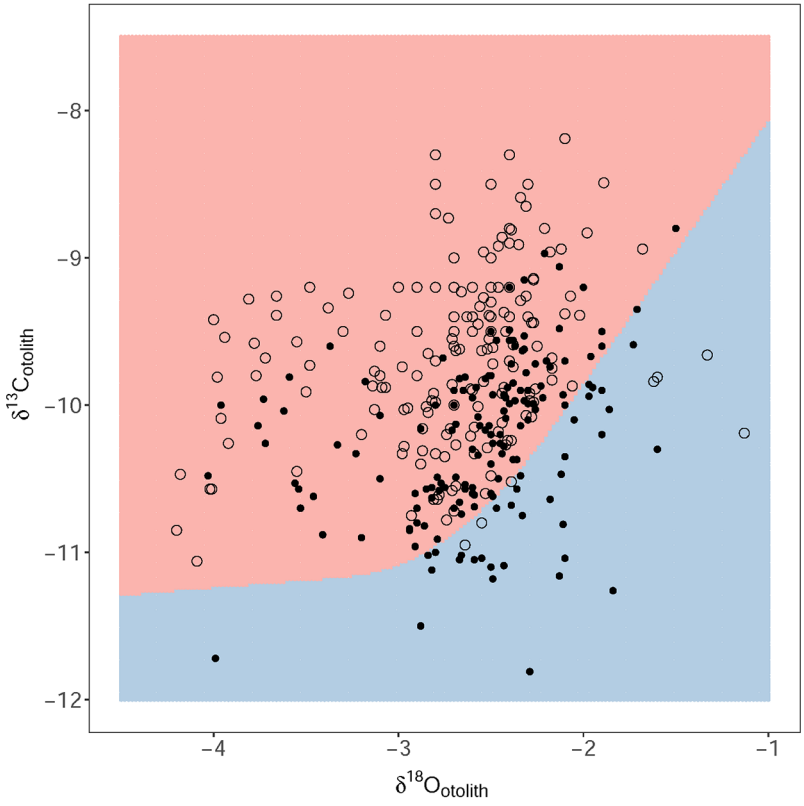

Fig. 8. As in Fig. 7, but for large juvenile yellowfin tuna

2008 (−10.56 to −9.66) from 121 to 159° E (Wells et al. 2012), which was larger than that in the present study (0.41‰ from 145 to 165° E [−9.51 to −9.04]). Wells et al. (2012) showed an increasing trend in $\delta^{18}O_{otolith}$ of yellowfin from 120° E to 160° W in the tropical and sub-tropical areas of the Pacific Ocean. The difference in $\delta^{18}O_{otolith}$ between the Philippines and Solomon Islands was 0.17‰ in 2008 (−2.82 to −2.65) from 121 to 159° E (Wells et al. 2012). This result was identical to that of the present study, which was 0.17‰ from 145 to 165° E (−2.64 to −2.37). A 0.12‰ increase in $\delta^{18}O_{seawater}$ from the west (10° S to 20° N and 140 to 150° E, n = 84 observations) to the east (10° S to 20° N and 160 to 170° E, n = 21) was found on the basis of the Global Seawater Oxygen-18 Database (Schmidt et al. 1999). Regarding latitudinal changes, a previous study showed a negative relationship between ambient temperature and $\delta^{18}O_{otolith}$ (Høie et al. 2004). In the western Pacific Ocean, the observation of $\delta^{13}C_{seawater}$ (120 to 180° E and 20° S to 45° N) revealed a decreasing trend (Schmittner et al. 2017), which matched the small juvenile $\delta^{13}C_{otolith}$ distribution from TROP and TEM in this study. Therefore, the assumption for the discriminant analysis of small juveniles is met with regard to $\delta^{13}C_{otolith}$ (e.g. small juvenile specimens were collected from their hatch areas). The food intake of animals at low latitudes tends to show larger $\delta^{13}C$ values because of the negative relationship between the sampling latitude and $\delta^{13}C_{plankton}$ (Rau et al. 1982).

The principal surface currents comprising the equatorial current system in the Pacific Ocean include the North Equatorial Current (NEC), the South Equatorial Current (SEC), and the North Equatorial Countercurrent. A subsurface equatorial undercurrent is also observed (Cromwell 1958). Considerable changes in surface and subsurface current conditions related to strong and weak easterly trade winds are known as the El Niño–Southern Oscillation (Amador et al. 2006). During El Niño, the flows in the NEC and SEC from east to west are weakened, causing warm surface water in the western Pacific Ocean to move to the east. El Niño and La Niña considerably change the oceanographic conditions in the sea surface layer; thus, during El Niño, purse seine and longline fishing grounds tend to move to the east because of the easterly movement of warm water in the sea surface layer (Lehodey et al. 1997, Williams & Reid 2019, Satoh et al. 2021). In this study, large juveniles were primarily caught by purse seine fisheries in TROP. El Niño occurred in 2014 and 2015, which induced fish movements; therefore, some large juvenile specimens caught in the eastern part in these 2 years possibly moved from the west, which reduced the differences in stable isotopes between the east and west. Thus, the oceanographic conditions affected the longitudinal changes in stable isotopes. Moreover, La Niña occurred in 2008, which may introduce further annual differences. However, this finding is not the case for $\delta^{18}O_{otolith}$. The annual differences in sea temperature significantly decreased in 2014 and 2015 (El Niño year) compared with other years in TROP. The redistribution of fish derived from large-scale oceanographic conditions may cause annual differences in stable isotopes.

4.2. Relationship between oceanographic conditions and stable isotopes

The oceanographic conditions were observed using a CTD probe at each sampling station, which en-

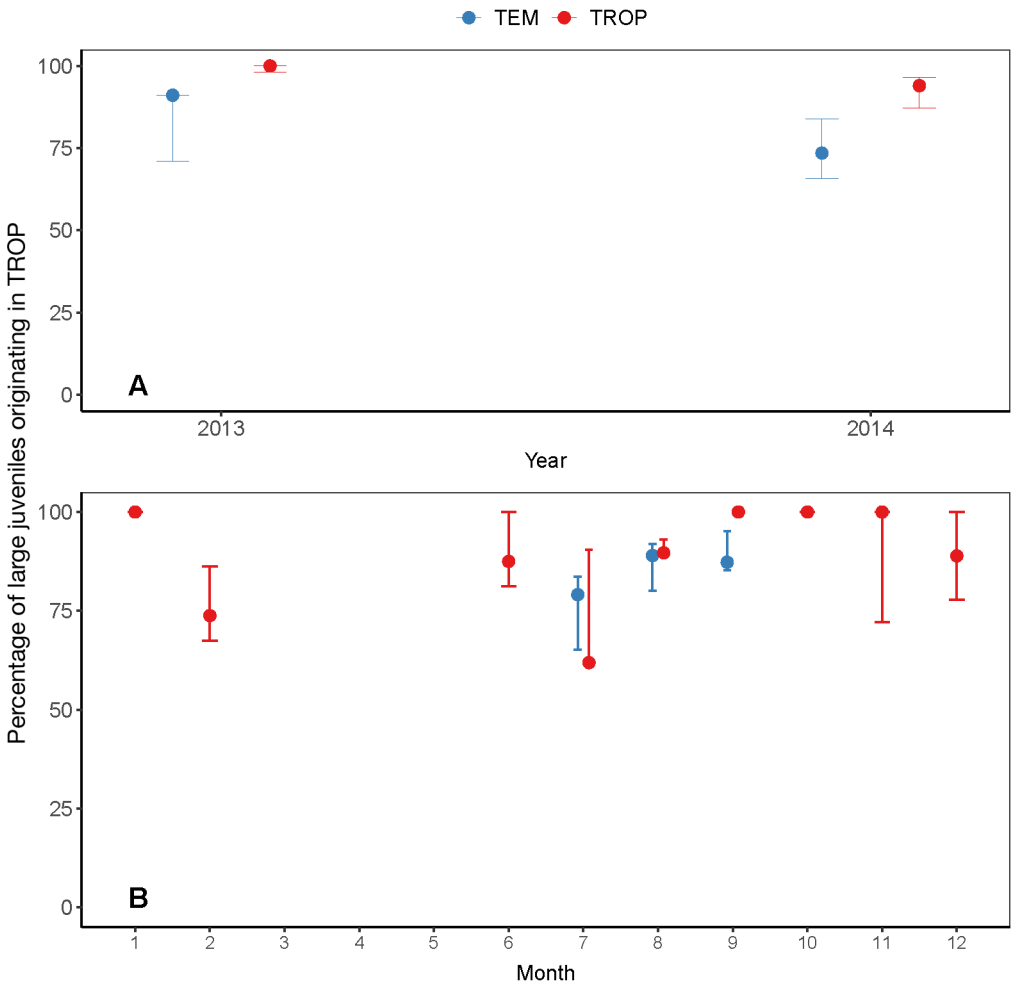

Fig. 9. Area-specific (A) annual and (B) monthly changes in the percentage of large juvenile yellowfin tuna *Thunnus albacares* originating from tropical areas (TROP) in the western and central Pacific Ocean. Error bars: SE

abled correlation analyses between the oceanographic conditions and stable isotopes in this study. Previous studies reported a positive relationship between salinity and $\delta^{13}C_{otolith}$ (a tank experiment for black bream: Elsdon & Gillanders 2002; white perch in an estuary environment: Kerr et al. 2007), which matched the results of the present study. However, a strong negative correlation between salinity and $\delta^{13}C_{otolith}$ was reported for Atlantic herring (Macdonald et al. 2020). The relationship between water temperature and $\delta^{13}C_{otolith}$ is inconsistent among studies (Elsdon & Gillanders 2002), particularly the slope (negative relationship: a wide range of fish species: Kalish 1991; Atlantic croaker: Thorrold et al. 1997; Elsdon & Gillanders 2002, Kerr et al. 2007; Atlantic herring: Macdonald et al. 2020; positive relationship: mollusk, Grossman & Ku 1986). Thorrold et al. (1997) also noted that a positive relationship between water temperature and $\delta^{13}C_{otolith}$ was masked to a degree by a positive correlation between delta ^{13}C ($\delta^{13}C_{otolith} - \delta^{13}C_{seawater}$) and somatic growth and otolith precipitation rates. In this study, $\delta^{13}C_{otolith}$ was lower in TEM than in TROP. A previous study showed that 10–30 % of the carbon in otoliths may be derived from metabolic sources, indicating a dietary origin. Otolith carbon may also come from dissolved inorganic carbon in the water (Campana 1999).

A positive relationship was observed between salinity and $\delta^{18}O_{otolith}$ (Kerr et al. 2007; cod: Høie et al. 2004), which was inconsistent with this study. However, the relationship between salinity and $\delta^{18}O_{otolith}$ is inconsistent among studies (positive relationship — Kerr et al. 2007; cod: Høie et al. 2004; yellowfin tuna: small juveniles in this study; negative relationship — Macdonald et al. 2020; yellowfin tuna: large juveniles in this study). $\delta^{18}O_{otolith}$ depletes more with increasing sea temperature (Kalish 1991, Thorrold et al. 1997, Elsdon & Gillanders 2002, although

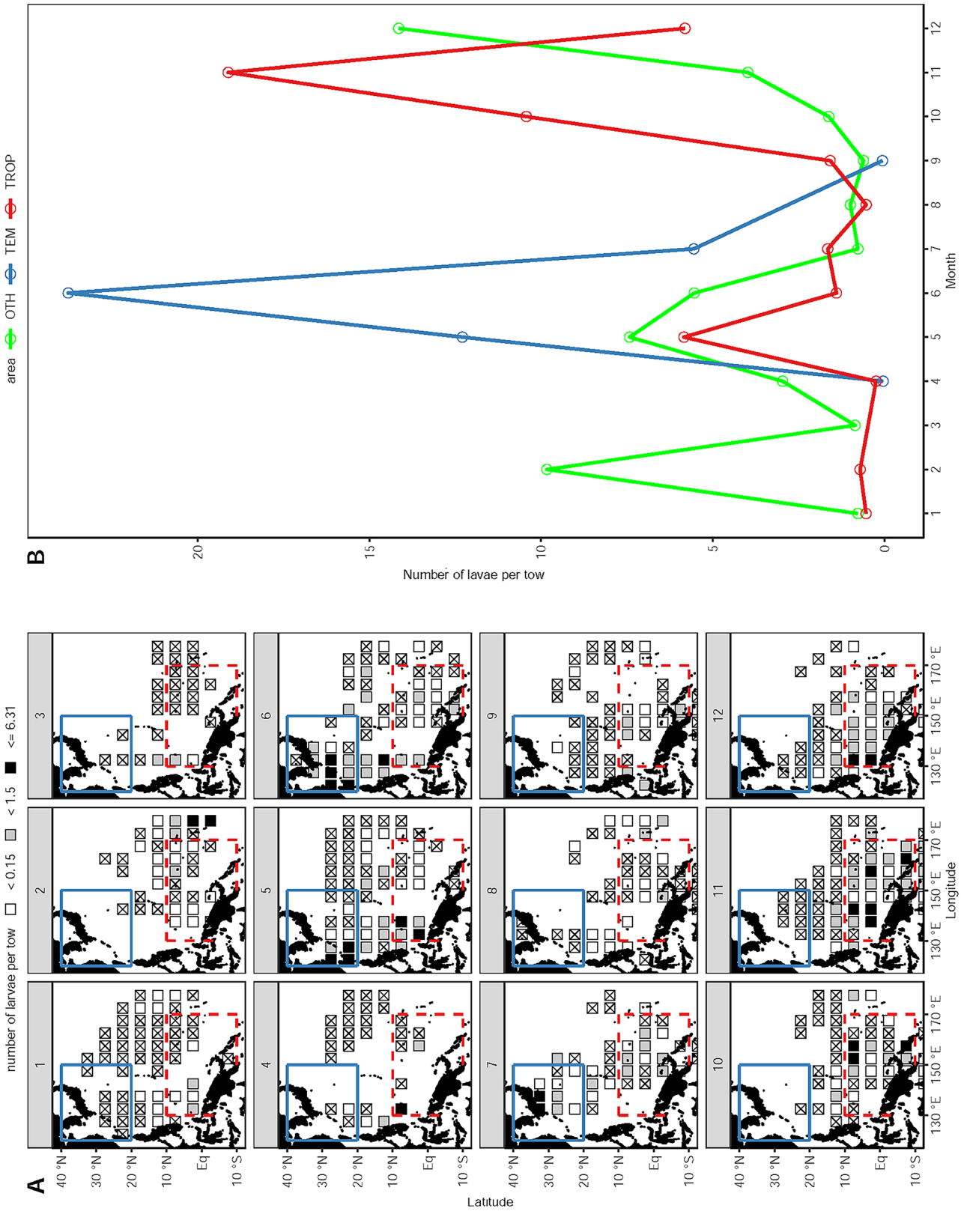

Fig. 10. (A) Monthly geographical distributions of the number of plankton net tows and number of yellowfin tuna larvae per plankton net tow. Crosses indicate no larval catch, even though more than 10 plankton net tows occurred per month. Blue solid and red dashed lines indicate the temperate (TEM) and tropical (TROP) areas, respectively. (B) Monthly changes in the number of yellowfin tuna larvae per plankton net tow by area based on the Japan Fisheries Research and Education Agency larval database. The green line indicates areas other than TROP and TEM. OTH: other areas

Table 4. Results of sensitivity analyses for the 2 scenarios of the specimen standard length (SL) range to understand the effect of fish size on the classification success rate and mixing rate of discriminant analyses. Scenario 1: 5–40 cm SL; Scenario 2: <12 and >25 cm SL. The classification success rate (%) for small juveniles and the percentage of large juveniles originating from the tropical areas (%) (mixing rate) by area and year sampled are based on a general additive model. TEM: temperate; TROP: tropical areas other than TROP and TEM

Sampling area	Sampling year	Scenario 1		Scenario 2	
		N	Classification success rate (%)/mixing rate (%)	N	Classification success rate (%)/mixing rate (%)
Small juveniles	Overall	82	91.5	162	92.0
TEM	All years	30	83.3	24	66.7
TEM	2011	15	80.0	12	58.3
TEM	2012	15	86.7	12	75.0
TROP	All years	52	96.2	138	96.5
TROP	2012	15	100.0	35	100.0
TROP	2013	37	94.6	78	94.9
Large juveniles	Overall	321	90.3	302	92.0
TEM	All years	149	83.2	130	86.9
TEM	2013	32	100.0	44	90.9
TEM	2014	117	78.6	86	84.9
TROP	All years	172	96.5	172	95.9
TROP	2013	55	100.0	55	100.0
TROP	2014	117	94.9	117	94.0

the trend is nonlinear; yellowfin tuna; Wells et al. 2012; Macdonald et al. 2020), which is similar to the results of this study. Compared with carbon, ambient water is considered the primary source of oxygen in otoliths (Campana 1999). If the effect of temperature on $\delta^{18}O_{otolith}$ is larger than that of salinity in the TEM, then it can introduce a higher $\delta^{18}O_{otolith}$ than the expected value in a low-salinity environment. We cannot isolate the influence of sea temperature or salinity from other unquantified factors (e.g. pH and ambient water concentrations) among these sampling stations; thus, any relationships in these results must be viewed as correlative only.

4.3. Construction of an indicator of nursery grounds

The classification success rate was as high as 90.7%, which is considered a useful indicator. The lower success rate in TEM (72.2%) than in TROP (96.5%) partially reflects the sample size. Although the success rate was high, there is still concern about the samples being representative of the WCPO yellowfin population. The question is whether the limited sampling season (TEM: June and July; TROP: November and December) for small juveniles is representative of this stock. Yellowfin tuna larvae occur year-round in tropical areas,

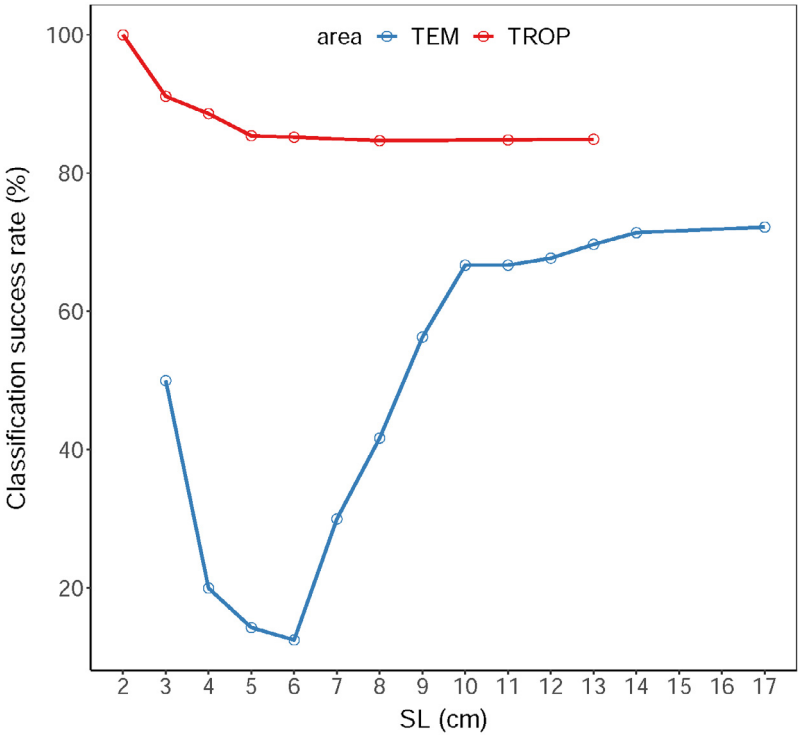

Fig. 11. Changes in the classification success rate of the classification model based on the standard length (SL) ranging from 2 to 18 cm

and their distribution expands to temperate areas during summer in the Northern and Southern Hemispheres of the WCPO (e.g. Ueyanagi 1969, Nishikawa et al. 1985, Suzuki 1994). The low temperature limit of the larval distribution of yellowfin tuna was assumed to be approximately 24°C, with some exceptions (Suzuki 1994). In an experiment on artificially fertilized yellowfin eggs, the highest rate of occurrence of normally hatched larvae was observed at an average water temperature of 26.4–27.8°C, but no normal larvae were found in a temperature range below 18.7°C or above 31.9°C (Harada et al. 1980). Larval distribution, which indicates spawning success of this species, is strongly controlled by sea temperature changes. In contrast, an analysis of spawning potential (product of fecundity, rate of group maturity, sex ratio, and abundance index) using specimens caught by longline vessels showed a seasonal peak in December to January in the western tropical Pacific (120 to 180° E) (Kikawa 1966). This seasonality in tropical areas was also supported by larval density analysis in this study (Fig. 10). The peak spawning season and sampling season in this study in TROP matched. Small juveniles were sampled during the season of larval abundance when the majority of larvae occurred in each area, indicating that the small juvenile samples used for this analysis are representative of each area.

In this study, larval density analysis indicated that our study coverage decreased to around 40% when considering the whole WCPO range (west of 180°). In particular, areas close to the Philippines, a potential spawning area and nursery ground, were not covered in this study. Tagging experiments in TEM revealed that a number of yellowfin tuna released in the southern part of TEM were recaptured near Philippine waters (Matsumoto et al. 2013). There was a large catch of small yellowfin in Philippine waters (Langley et al. 2011, Vincent et al. 2020a,b), and there was a high larval density in April and May in this region (Fig. 10). Philippine waters are characterized by low salinity (~34 psu) and high sea temperature (~30°C) (Gordon et al. 2011), which are different from the oceanographic conditions of TEM (34.1 psu, 27°C) and TROP (34.5 psu, 28.8°C). Wells et al. (2012) reported a lower $\delta^{13}C_{otolith}$ (−10.5 to −9.8) and $\delta^{18}O_{otolith}$ (−2.82 to −2.65) values of large juveniles (as defined in the current study) in Philippine waters relative to other tropical and sub-tropical areas of the Pacific Ocean. Therefore, it can be assumed that some small juveniles that originated from Philippine waters may migrate to TEM, while some large juveniles caught in TEM that were classified initially to originate from TROP might come from the Philippines instead. The incorporation of small juvenile samples from the Philippine archipelago is needed to enhance understanding of the population connectivity of yellowfin tuna. Samples from areas east of 180° W and during winter are also absent. Given the otolith stable isotope ratios of previous studies, the samples caught in the eastern area are expected to be distributed in the upper right area of the partition plane (Figs. 7 & 8), increasing the classification ability of the analysis.

Related to the Scenario (1) of the sensitivity tests, the relationship between the stable isotopes and SL for the smallest group (<5 cm SL) and largest group (>40 cm SL) did not affect the classification rates and mixing rates. The result of the Scenario (2) and the comparison of SL of the matched and mis-matched groups indicate that the assumption for the construction of the indicator (e.g. small juvenile specimens were collected from their hatch areas) is not violated, although no conclusive results were found for the starting point of migration of small juveniles to the other areas from the third scenario.

4.4. Mixing rate between the areas of large juveniles

An assessment of this stock (Vincent et al. 2020a) revealed a proportional distribution of total biomass (by weight) in each region apportioned by the source region of yellowfin tuna. The high percentage (78.4%) of tropical origin for large juveniles in the TEM was estimated in this study, which is different from the very low percentage in the stock assessment results in the WCPO (Fig. 27 in Vincent et al. 2020a). On the other hand, in this study, the majority (95.9%) of the large juveniles in TROP were from tropical origins, which is similar to that of the stock assessment. Migration patterns between TEM and TROP in this stock assessment were set up using tagging experiment results after recruitment, presenting regional fidelity. The very low percentage of tropical-origin fish in TEM may result in overestimation of abundance to explain catch in this area if they do not return to TROP after they mature. This study found active population connectivity before recruitment, especially from TROP to TEM, which can contribute to the establishment of a precise stock assessment model for this species. However, we also need to further investigate the migration traits of large, mature fish in TEM. If large fish migrate to the TROP to spawn, this may lead to consistent stock assessment results.

The point estimates of the percentage in TROP were always higher than those in TEM in all sampled years (Table 3, Fig. 9). The percentage in TROP from April to September was slightly lower than that in other months, suggesting seasonal movement of this species, which could be more active in the warmer season.

4.5. Conceptual model for population connectivity before recruitment in the two areas

The stable isotopes for small and large juveniles between TEM and TROP were compared. If there is no mixing between the areas from small to large juveniles as they grow, then the distribution of the isotope values will be identical for the 2 fish size categories in each area. However, we found large differences in the distribution of stable isotope values between small and large juveniles in the 2 areas. The stable isotope patterns were still detected in each sampling year. These results indicate that mixing of yellowfin tuna occurred between TEM and TROP before they reached a size where they are captured in fisheries.

In addition, no clear migration pattern has been reported for yellowfin tuna in the western Pacific Ocean, such as the trans-ocean migration of other tuna species such as albacore (Ichinokawa et al. 2008). Tagging experiments for yellowfin tuna revealed that most recaptures occurred near the release points even after a long time at liberty (Langley et al. 2011, Vincent et al. 2020a,b). Of 12 707 yellowfin tuna tagged near Japan, 516 were recaptured near Japan and 14 came from tropical areas. Of 66 477 yellowfin tuna tagged in the tropical areas of the WCPO, only 3 fish were recaptured near Japan (2005 to 2009, Pacific Tuna Tagging Program) (Langley et al. 2011). Most yellowfin tuna tend to remain near the place where they were tagged despite a number of long-distance migrations of over 1000 n miles (Langley et al. 2011, Vincent et al. 2020 a, b). Tagging experiments in the southern area of the TEM for young fish (30–40 cm FL) revealed 2 migration paths; most fish move to the Japanese Pacific side along the Kuroshio Current, whereas some fish move to the southern area, including the tropical areas of the western Pacific Ocean (Matsumoto et al. 2013). Numerous tagging experiments suggest that the connectivity of yellowfin tuna between TEM and TROP is limited based on tagging of fish larger than approximately 30 cm FL after recruitment.

For narrow-barred Spanish mackerel *Scomberomorus commerson* in the waters of northern and western Australia, Buckworth et al. (2007) proposed a metapopulation structure with adult assemblages linked by larval dispersal (Moore et al. 2020). Such population connectivity through dispersal during the early life history of yellowfin tuna was discussed in Buckworth et al. (2007). Spawning in the TROP can occur year-round, but it also shows seasonality with the main spawning during the northern hemisphere winter months. Some hatched larvae are thought to migrate to temperate areas before recruitment (<30 cm SL, about 3 mo after hatching). Therefore, fish growth can occur in the cooler sea temperature environment encountered if hatching occurs in December in TROP. When they are spawned, the SST (30–90 m, layer sampled for small juveniles) is approximately 28°C, except during El Niño; they then migrate to TEM within 2 or 3 mo after hatching. The SST (5–35 m) from February to March is approximately 21°C. A tank experiment for yellowfin tuna larvae and juveniles reported that the temperature suitable for a normal larval development ranged from 18.7°C to 31.0°C, and small juveniles were able to survive up to 49 d after hatching (Japan Sea Farming Association 1996). Therefore, sea temperature conditions are highly suitable for the growth of this species if they stay in the surface layer, although they migrate from TROP to TEM. The migration path from TROP to TEM could be over a 4000 km path by utilizing the NEC (around 10° N, westward in TROP) and the Mindanao Current (MC, around 125° E, 10–20° N) to reach the southern part of TEM. The mean zonal velocities of the NEC and MC are approximately 30 cm s^{-1} (at a depth of 70 m) (Zhang et al. 2017) and 1.3 m s^{-1} (at a depth of approximately 100 m), respectively. The total period of travel from TROP to TEM when a fish moves at the mean velocity of each current is about 72 d (from 10° N, 140° E to 23° N, and from 10° N, 126° E to 124° N). The sea temperature conditions and sea current velocity in this study area support the hypothesis of dispersal from TROP to TEM. An early-stage field survey to track a drift buoy for tuna larval high-density patches indicated that some individuals migrated long distances along the ocean currents before recruitment from a hatching area to a recruitment area (Davis et al. 1991, Satoh 2010, Satoh et al. 2013). Although the path from TEM to TROP for larval dispersal is unclear, we have proposed a conceptual model for population connectivity thorough dispersal during early life history (e.g. before

recruitment) between TEM and TROP, particularly from TROP and TEM in WCPO.

In summary, the large differences in the distribution of stable isotopes between small and large juveniles in the 2 study areas indicated that mixing of yellowfin tuna occurred between TEM and TROP before reaching sizes captured in fisheries. A conceptual model for population connectivity before recruitment is proposed from TROP and TEM in WCPO, which can inform the development of stock assessment models of yellowfin tuna in this region.

Acknowledgements. We especially thank Captain K. Hata and the crew of the 'Shunyo-Maru' for their useful suggestions and constant support, and we thank Dr. H. Ashida, Dr. K. Watanabe, and Dr. H. Ijima for support during the research cruises. We appreciate the support of SI Science and the GEO-Science Laboratory in the analysis of stable isotopes. We are grateful for suggestions regarding the treatment of otolith powder given by Dr. S. Sakai of JAMSTEC and S. Matsuda of IzumoWeb LPC. We thank numerous individuals for assistance in otolith collections, including the staff of Yaizu, Makurazaki, and Yamagawa fish markets; staff of OFCF; and staff of Japan Far Seas Purse Seine Fishing Association and Yamasan Nishikawa. We appreciate Dr. M. Okazaki and D. Inagake of the FRA. We also thank Dr. M. Ogura and Dr. H. Minami for their suggestions and extensive support to complete this study. Funding for this work was provided by a research and assessment program for internationally managed fisheries resources, the Fisheries Agency of Japan. Comments from anonymous reviewers and the editor improved this manuscript.

LITERATURE CITED

Amador JA, Alfaro EJ, Lizano OG, Magaña VO (2006) Atmospheric forcing of the eastern tropical Pacific: a review. Prog Oceanogr 69:101–142

Bayliff WH (1979) Migrations of yellowfin tuna in the eastern Pacific Ocean as determined from tagging experiments initiated during 1968–1974. Bull IATTC 17: 447–506

Bayliff WH (1984) Migrations of yellowfin and skipjack tuna released in the central portion of the eastern Pacific Ocean, as determined by tagging experiments. IATTC Intern Rep 18:1–108

Buckworth RC, Newman SJ, Ovenden JR, Lester RJG, McPherson GR (2007) The stock structure of northern and western Australian Spanish mackerel. Final Report, Fisheries Research & Development Corporation project 1998/159. Department of Primary Industry, Fisheries and Mines, Northern Territory Government, Darwin

Campana SE (1999) Chemistry and composition of fish otoliths: pathways, mechanisms and applications. Mar Ecol Prog Ser 188:263–297

Chen M, Guo L, Ma Q, Qiu Y, Zhang R, Lv E, Huang Y (2006) Zonal patterns of $\delta^{13}C$, $\delta^{15}N$, and ^{210}Po in the tropical and subtropical North Pacific. Geophys Res Lett 33: L04609

Cromwell T (1958) Thermocline topography, horizontal currents and ridging in the eastern tropical Pacific. Bull IATTC 3:135–164

Davis TLO, Lyne V, Jenkins GP (1991) Advection, dispersion and mortality of a patch of southern bluefin tuna larvae *Thunnus maccoyii* in the East Indian Ocean. Mar Ecol Prog Ser 73:33–45

Elsdon TS, Gillanders BM (2002) Interactive effects of temperature and salinity on otolith chemistry: challenges for determining environmental histories of fish. Can J Fish Aquat Sci 59:1796–1808

Gordon AL, Sprintall J, Ffield A (2011) Regional oceanography of the Philippine Archipelago. Oceanography 24: 14–27

Grossman EL, Ku TL (1986) Oxygen and carbon isotope fractionation in biogenic aragonite: temperature effects. Chem Geol 59:59–74

Hampton J, Fournier DA (2001) A spatially disaggregated, length-based, age-structured population model of yellowfin tuna (*Thunnus albacares*) in the western and central Pacific Ocean. Mar Freshw Res 52:937–963

Hampton J, Gunn J (1998) Exploitation and movements of yellowfin tuna (*Thunnus albacares*) and bigeye tuna (*T. obesus*) tagged in the north-western Coral Sea. Mar Freshw Res 49:475–489

Harada T, Miyashita S, Yoneshima H (1980) Effect of water temperature on yellowfin tuna hatching. Bull Fac Agric Kinki Univ 13:29–32

Higashi R, Sakuma K, Chiba SN, Suzuki N and others (2016) Species and lineage identification for yellowfin *Thunnus albacares* and bigeye *T. obesus* tunas using two independent multiplex PCR assays. Fish Sci 82:897–904

Høie H, Otterlei E, Folkvord A (2004a) Temperature-dependent fractionation of stable oxygen isotopes in otoliths of juvenile cod (*Gadus morhua* L.). ICES J Mar Sci 61: 243–251

Ichinokawa M, Coan AL, Takeuchi Y (2008) Transoceanic migration rates of young North Pacific albacore, *Thunnus alalunga*, from conventional tagging data. Can J Fish Aquat Sci 65:1681–1691

Itano D, Holland K (2000) Movement and vulnerability of bigeye (*Thunnus obesus*) and yellowfin tuna (*Thunnus albacares*) in relation to FADS and natural aggregation points. Aquat Living Resour 13:213–223

Japan Sea Farming Association (1996) Yellowfin tuna. Annual report. Japan Sea Farming Association, Tokyo

Kalish JM (1991) Oxygen and carbon stable isotopes in the otoliths of wild and laboratory reared Australian salmon (*Arripis trutta*). Mar Biol 110:37–47

Kaltongga B (1998) Regional Tuna Tagging Project: data summary. Tech Rep 35. Oceanic Fisheries Programme, Secretariat of the Pacific Community, Noumea

Kerr LA, Secor DH, Kraus RT (2007) Stable isotope ($\delta^{13}C$ and $\delta^{18}O$) and Sr/Ca composition of otoliths as proxies for environmental salinity experienced by an estuarine fish. Mar Ecol Prog Ser 349:245–253

Kikawa S (1966) The distribution of maturing bigeye and yellowfin and an evaluation of their spawning potential in different areas in the tuna longline grounds in the Pacific. Rep Nankai Reg Fish Res Lab 23:131–208

Langley A, Hoyle S, Hampton J (2011) Stock assessment of yellowfin tuna in the western and central Pacific Ocean. Western and Central Pacific Fisheries Commission, Scientific Committee 7th Session: WCPFC-SC7-2011/ SA WP-03

LeGrande AN, Schmidt GA (2006) Global gridded data set of the oxygen isotopic composition in seawater. Geophys Res Lett 33:L12604

Lehodey P, Bertignac M, Hampton J, Lewis A, Picaut J (1997) El Niño southern oscillation and tuna in the western Pacific. Nature 389:715–718

Macdonald JI, Drysdale RN, Witt R, Cságoly Z, Marteinsdóttir G (2020) Isolating the influence of ontogeny helps predict island-wide variability in fish otolith chemistry. Rev Fish Biol Fish 30:173–202

Matsumoto T, Kitagawa T, Kimura S, Semba Y and others (2013) Movement and behavior of tunas in relation with anchored fish aggregation devices (FADs) in the Nansei Islands Area. J Fish Eng 50:43–49

Moore BR, Bell JD, Evans K, Farley J and others (2020) Defining the stock structures of key commercial tunas in the Pacific Ocean. I. Current knowledge and main uncertainties. Fish Res 230:105525

Nishikawa Y, Honma M, Ueyanagi S, Kikawa S (1985) Average distribution of larvae of oceanic species of scombrid fishes, 1956–1981. Bull Natl Res Inst Far Seas Fish Lab 12:1–99

Okiyama M (1988) An atlas of the early stage fishes in Japan. Tokai University Press, Tokyo

Olson CL (1974) Comparative robustness of six tests in multivariate analysis of variance. J Am Stat Assoc 69:894–908

R Core Team (2021) R: a language and environment for statistical computing. R Foundation for Statistical Computing, Vienna

Rau GH, Sweeney RE, Kaplan IR (1982) ^{13}C:^{12}C ratio changes with latitude: differences between northern and southern oceans. Deep-Sea Res 29:1035–1039

Rooker JR, Secor DH, Zdanowicz VS, Itoh T (2001) Discrimination of northern bluefin tuna from nursery areas in the Pacific Ocean using otolith chemistry. Mar Ecol Prog Ser 218:275–282

Rooker JR, Secor DH, De Metrio G, Schloesser R, Block BA, Neilson JD (2008) Natal homing and connectivity in Atlantic bluefin tuna populations. Science 322: 742–744

Rooker JR, Wells RJD, Itano DG, Thorrold SR, Lee JM (2016) Natal origin and population connectivity of bigeye and yellowfin tuna in the Pacific Ocean. Fish Oceanogr 25: 277–291

Satoh K (2010) Horizontal and vertical distribution of larvae of Pacific bluefin tuna *Thunnus orientalis* in patches entrained in mesoscale eddies. Mar Ecol Prog Ser 404: 227–240

Satoh K, Tanaka Y, Masujima M, Okazaki M, Kato Y, Shono H, Suzuki K (2013) Relationship between the growth and survival of larval Pacific bluefin tuna, *Thunnus orientalis*. Mar Biol 160:691–702

Satoh K, Xu H, Minte-Vera CV, Maunder MN, Kitakado T (2021) Size-specific spatiotemporal dynamics of bigeye tuna (*Thunnus obesus*) caught by the longline fishery in the eastern Pacific Ocean. Fish Res 243:106065

Schaefer KM, Fuller DW (2022) Horizontal movements, utilization distributions, and mixing rates of yellowfin tuna (*Thunnus albacares*) tagged and released with archival tags in six discrete areas of the eastern and central Pacific Ocean. Fish Oceanogr 31:84–107

Schmidt GA, Biggs GR, Rohling EJ (1999) Global seawater oxygen 18 database, version 1.22. NASA Goddard Institute for Space Studies. https://data.giss.nasa.gov/o18data/

Schmittner A, Gruber N, Mix AC, Key RM, Tagliabue A, Westberry TK (2017) Global compilation of carbon-13 measurements during 1990–2005 in dissolved inorganic carbon ($d^{13}C$_DIC) (NCEI Accession 0157698). [120° to 180°E and 20° S to 45° N]. NOAA NCEI Dataset. https://www.ncei.noaa.gov/metadata/geoportal/rest/metadata/item/gov.noaa.nodc%3A0157698/html

Shiao JC, Yui TF, Høie H, Ninnemann U, Chang SK (2009) Otolith O and C stable isotope compositions of southern bluefin tuna *Thunnus maccoyii* (Pisces: Scombridae) as possible environmental and physiological indicators. Zool Stud 48:71–82

Shiao JC, Wang SW, Yokawa K, Ichinokawa M, Takeuchi Y, Chen YG, Shen CC (2010) Natal origin of Pacific bluefin tuna *Thunnus orientalis* inferred from otolith oxygen isotope composition. Mar Ecol Prog Ser 420: 207–219

Suzuki Z (1994) A review of the biology and fisheries for yellowfin tuna (*Thunnus albacares*) in the western and central Pacific Ocean. In: Shomura RS, Majkowski J, Langi S (eds) Interactions of Pacific tuna fisheries. Papers on biology and fisheries. Tech Pap 336/2. FAO, Rome

Tanabe T (2002) Studies on the early life ecology of skipjack tuna, *Katsuwonus pelamis*, in the tropical western-north Pacific. Bull Fish Res Agency 3:63–132

Tanabe T, Niu K (1998) Sampling juvenile skipjack tuna, *Katsuwonus pelamis*, and other tunas, *Thunnus* spp., using midwater trawls in the tropical western Pacific. Fish Bull 96:641–646

Thorrold SR, Campana SE, Jones CM, Swart PK (1997) Factors determining $\delta^{13}C$ and $\delta^{18}O$ fractionation in aragonitic otoliths of marine fish. Geochim Cosmochim Acta 61:2909–2919

Ueyanagi S (1969) Observations on the distribution of tuna larvae in the Indo-Pacific Ocean with emphasis on the delineation of the spawning areas of albacore, *Thunnus alalunga*. Bull Far Seas Fish Res Lab 2:177–203

Vincent M, Ducharme-Barth N, Hamer P, Hampton J, Williams P, Pilling G (2020a) Stock assessment of yellowfin tuna in the western and central Pacific Ocean. Western and Central Pacific Fisheries Commission, Scientific Committee 16th Session: WCPFC-SC16-2020/SA-WP-04 (Rev.3)

Vincent N, Ducharme-Barth N, Hamer P (2020b) Background analyses for the 2020 stock assessments of bigeye and yellowfin tuna. Western and Central Pacific Fisheries Commission, Scientific Committee 16th Session: WCPFC-SC16-2020/SA-IP-06. https://meetings.wcpfc.int/file/7865/download

Wells RJD, Rooker JR, Itano DG (2012) Nursery origin of yellowfin tuna in the Hawaiian Islands. Mar Ecol Prog Ser 461:187–196

Western and Central Pacific Fisheries Commission (2017) Summary report. Thirteenth regular session of the scientific committee. The Commission for the Conservation and Management of Highly Migratory Fish Stocks in the Western and Central Pacific Ocean. Rarotonga, Cook Islands, 9–17 August 2017

Wexler JB, Chow S, Wakabayashi T, Nohara K, Margulies D (2007) Temporal variation in growth of yellowfin tuna (*Thunnus albacares*) larvae in the Panama Bight, 1990–97. Fish Bull 105:1–18

Williams P, Reid C (2019) Overview of tuna fisheries in the western and central Pacific Ocean, including economic conditions, 2018. Western and Central Pacific Fisheries Commission 15th Regular Session of Scientific Committee WCPFC-SC15-2019/GN WP-1. https://meetings.wcpfc.int/node/11211

Williams P, Ruaia T (2021) Overview of tuna fisheries in the western and central Pacific Ocean, including economic conditions –2020. The western and central Pacific Fisheries Committee, Scientific committee seventeenth regular session: WCPFC-SC17-2021/GN-IP-1. https://meetings.wcpfc.int/file/9089/download

Yeo IK, Johnson R (2000) A new family of power transformations to improve normality or symmetry. Biometrika 87:954–959

Zhang L, Wang FJ, Wang Q, Hu S, Wang F, Hu D (2017) Structure and variability of the North Equatorial Current/undercurrent from mooring measurements at 130° E in the western Pacific. Sci Rep 7:46310

Editorial responsibility: Alistair Hobday, Hobart, Tasmania, Australia
Reviewed by: 3 anonymous referees

Submitted: September 5, 2022
Accepted: May 11, 2023
Proofs received from author(s): June 20, 2023